Model uncertainty in non-linear numerical analyses of slender reinforced concrete members

MODEL UNCERTAINTY IN NON-LINEAR NUMERICAL ANALYSES OF SLENDER REINFORCED CONCRETE MEMBERS

Diego Gino[1], Paolo Castaldo[1], Luca Giordano[1], Giuseppe Mancini[1]

[1]Department of Structural, Geotechnical and Building Engineering (DISEG), Politecnico di Torino, Turin, Italy. E-mail: paolo.castaldo@polito.it; diego.gino@polito.it; luca.giordano@polito.it; giuseppe.mancini@polito.it

Corresponding Author

Gino Diego

diego.gino@polito.it

+39 0110905307

MODEL UNCERTAINTY IN NON-LINEAR NUMERICAL ANALYSES OF SLENDER REINFORCED CONCRETE MEMBERS

Diego Gino[1], Paolo Castaldo[1], Luca Giordano[1], Giuseppe Mancini[1]

[1]Department of Structural, Geotechnical and Building Engineering (DISEG), Politecnico di Torino, Turin, Italy. E-mail: paolo.castaldo@polito.it; diego.gino@polito.it; luca.giordano@polito.it; giuseppe.mancini@polito.it

ABSTRACT

The present study aims to characterize the epistemic uncertainty within the use of global non-linear numerical analyses (i.e., NLNAs) for design and assessment purposes of slender reinforced concrete (RC) members. The epistemic uncertainty associated to NLNAs may be represented by approximations and choices performed during the definition of a structural numerical model. In order to quantify epistemic uncertainty associated to a non-linear numerical simulation, the resistance model uncertainty random variable has to be characterized by means of the comparison between experimental and numerical results. With this aim, a set of experimental tests on slender reinforced concrete columns known from the literature is considered. Then, the experimental results in terms of maximum axial load are compared to the outcomes achieved from NLNAs. Nine different modelling hypotheses are herein considered to characterize the resistance model uncertainty random variable. The probabilistic analysis of the results has been performed according to Bayesian approach accounting also for both the previous knowledge from the scientific literature and the influence of the experimental uncertainty on the estimation of the statistics of the resistance model uncertainty random variable. Finally, the resistance model uncertainty partial safety factor is evaluated in line with the global resistance format of *fib* Model Code for Concrete Structures 2010 with reference to new and existing RC structures.

KEYWORDS: NLNAs; safety formats; global resistance; slender columns; reinforced concrete structures, resistance model uncertainty.

1. INTRODUCTION

The use of non-linear numerical analyses (i.e., NLNAs) to design and assess both new and existing reinforced concrete (RC) structures and buildings is one of the most important development of the last decades for structural engineers and practitioners. With the advances in computer-assisted design tools, more and more structures are likely to be designed and assessed by means of non-linear numerical analyses in the near future. For instance, over the years, several guidelines [1],[2] and appropriate methodologies [3]-[6] have been defined in order to finalize structural verifications by means of NLNAs. Moreover, the next generation of design codes for practice will make possible to use such kind of refined methods and, for this reason, an in-depth investigation of the related uncertainties is needed from researchers. The NL numerical simulations turn out to be an efficient tool to perform the assessment/design of RC structures having complex geometry (e.g., irregular storeys configuration in buildings), geometrical and mechanical non-linearity, poor detailing and local damaging (e.g., localized cracking in members and damage in nodes of RC frames after accidental loading events). Concerning the applications of NLNAs to RC members affected by the geometrical non-linearity (in addition to the non-linearity associated to concrete and reinforcement steel material behaviour), several studies are reported in literature [7],[8] also investigating the effect of strengthening interventions [9] typically realized on columns of existing RC buildings.
The reliability analysis of reinforced concrete structures can be efficiently performed by means of NLNAs throughout the global resistance format approach in line with [10],[11]. The global resistance format allows to compare the design value of actions directly to the associated design value of the

global resistance of a structural system or component. The global structural resistance can be estimated using a NLNA and, its design value can be evaluated accounting for the influence of aleatory and epistemic uncertainties [12]-[13] through the definition of appropriate partial safety factors in line with pre-determined target levels of reliability distinguishing between new and existing structures [10]-[15]. The influence of the aleatory uncertainty and variability of the failure mode on the outcomes of reliability analysis performed by means of NLNAs has been investigated by [16],[17], as well as, the relevance and quantification of resistance model uncertainty (i.e., epistemic uncertainty) has been studied by [18]-[19]. However, the mentioned above investigations do not consider explicitly slender structural members significantly affected by geometrical non-linearity.
For instance, this study is focused on the evaluation and quantification of the epistemic uncertainty associated to NLNAs of RC members affected by significant geometrical non-linearities and of the associated partial safety factor within the global resistance format approach [10]. The general methodology proposed by [12]-[13] for quantification of the epistemic uncertainty in NLNAs is adopted and also extended in order to account for the literature knowledge. The epistemic uncertainty associated to NLNAs are represented by model simplifications, numerical approximations and choices performed during the definition of a structural model [12]-[13],[18],[20]. This kind of uncertainty does not include the aleatory uncertainty related to both materials and geometry. The quantification of the epistemic uncertainty associated to a non-linear numerical simulation can be performed through the assessment of the resistance model uncertainty random variable ϑ. The latter, can be characterized by means of the comparison between experimental and numerical results in terms of global resistance [21]. With this aim, 40 experimental tests on slender RC columns known from the scientific literature are considered [22]-[30]. The experimental results in terms of maximum axial load are compared to the outcomes achieved from appropriate NLNAs (specifically, finite element method and fiber models). In the present investigation, nine different modelling hypotheses are considered in order to characterize a comprehensive probabilistic model for the resistance model uncertainty random variable ϑ. As discussed in [12]-[13],[18], a specific modelling hypothesis for NLNAs collects choices related to material constitutive models, to the kinematic compatibility and to the equilibrium between internal and external forces. The probabilistic analysis of the results has been performed according to the Bayesian approach as proposed by [12]-[13], accounting also for the knowledge from the scientific literature [31] and the influence of the experimental uncertainty on the estimation of the statistics (i.e., mean value and variance) of the resistance model uncertainty random variable ϑ. In fact, the direct comparison between experimental and numerical results leads to an estimation of the resistance model uncertainty random variable ϑ which is inclusive of the uncertainties associated to the execution of the experiments. In general, the experimental uncertainty may be neglected if the coefficient of variation of the resistance model uncertainty random variable ϑ is higher than 10% [21] concerning test on non-corroded reinforced concrete members. However, for the case of members realized with reduced cross sections (i.e., around 15-20 cm concerning small dimensions), the influence of the experimental uncertainty on the statistical parameters for the resistance model uncertainty ϑ may be significant. Hence, the probabilistic calibration is herein performed considering both significant and negligible influence of the experimental uncertainty. Finally, the resistance model uncertainty partial safety factor γ_{Rd} is evaluated in line with the global resistance format of [9],[10] accounting for appropriate reliability differentiation for new/existing RC structures and the hypotheses of dominant or non-dominant random variable within the reliability analysis.

2. DEFINITION AND CHARACTERIZATION OF UNCERTAINTIES ACCORDING TO SAFETY FORMATS FOR NON-LINEAR NUMERICAL ANALYSES

The uncertainties which affect structural engineering have sources of different nature. Focusing on the uncertainties associated to resistance models, these sources are related both to the inherent randomness of geometrical characteristic of structural elements or of physical properties of materials

(e.g., concrete compressive strength and reinforcement yielding strength) and to missing knowledge, simplification and assumptions performed within the definition of the resistance model itself [12]-[13], [18]. In the literature [20]-[21],[32], the firsts are denoted, usually, as aleatory uncertainties while, the latter are recognized as the epistemic ones. Even if a strict distinction between the mentioned above families of uncertainties is not possible [20], it represents an efficient discrimination in order to include their effects in design code provisions [33]. In particular, concerning the use of NLNAs for design and assessment purposes, the studies [3],[10],[34] define appropriate safety formats which include efficiently both aleatory and epistemic uncertainties and their influence on the global structural response. With reference to the global resistance format [10],[16] and in line with the semi-probabilistic approach [33],[35], the design value of global structural resistance R_d can be compared to the design value of actions F_d under the specific disposition and combination according to the following expression:

$$R_d \geq F_d \tag{1}$$

The design value of actions F_d can be evaluated in line with specifications of [33] while, the design value of global structural resistance R_d can be evaluated through NLNAs according to the mentioned above safety formats [3],[10],[34] with reference to the following expression:

$$R_d = \frac{R_{NLNA}\left(x_{rep}\right)}{\gamma_R \gamma_{Rd}} \tag{2}$$

In Eq.(2), $R_{NLNA}(x_{rep})$ represents the global structural resistance evaluated by means of NLNAs using the representative values x_{rep} for geometrical and material properties in line with the selected safety format [3],[10],[34]. The level of structural reliability is involved by means of two different partial safety factors:

- the *global resistance safety factor* γ_R which takes into account, at the level of global structural behaviour, the influence of the aleatory uncertainties related to the material properties and even geometry. This partial safety factor can be determined in compliance with a specific target level of reliability according to the methodology described by the selected safety format [3],[10],[34];
- the *resistance model uncertainty safety factor* γ_{Rd} which takes into account the epistemic uncertainty related to definition of the non-linear numerical model; the design codes (i.e., [10],[36]) and scientific literature [12] report different propositions for this coefficient. This partial safety factor is horizontal and independent on the safety format [3],[10],[34] selected in order to carry out the structural verification.

The present investigation is focused on the characterization of the epistemic uncertainty associated to NLNAs of slender RC members and on the estimation of the appropriate global resistance model uncertainty safety factor γ_{Rd}. The epistemic uncertainty in NLNAs can be associated to "missing" knowledge, hypotheses and simplifications related to constitutive laws, kinematic compatibility and equilibrium of forces and to assumptions concerning auxiliary non-physical variables or individual choices [20], [12]-[13]. All the mentioned above aspects characterize the selection of a specific modelling hypothesis [12]-[13], also denoted in literature as "solution strategy" [18].

With reference to [32],[21], the epistemic uncertainty in resistance models may be exhaustively represented by the resistance model uncertainty random variable ϑ denoted as:

$$\vartheta \approx \frac{R_{Exp}\left(X,Y\right)}{R_{NLNA}\left(X\right)} \tag{3}$$

Eq.(3) relates the global resistance estimated from an experimental test $R_{Exp}(X,Y)$ to the global resistance estimated through a NLNA $R_{NLNA}(X)$. X is a vector of basic variables included into the

resistance model (i.e., NLN model), Y is a vector of variables that may affect the resisting mechanism but are neglected in the model and, their unknown influence, is indirectly incorporated including the random variable ϑ within the reliability analysis. As discussed by [12]-[13], an in-depth probabilistic characterization of the resistance model uncertainty random variable ϑ and of the related partial safety factor γ_{Rd} needs to be addressed in relation to the multiplicity of modelling hypotheses available to practitioners and engineers and the target reliability differentiation between new and existing structures. In line with the approach of [12]-[13], the calibration of the resistance model uncertainty safety factor γ_{Rd} may be performed according to the following steps:

1) *Selection of the benchmark experimental tests*: the selection of the benchmark set of experimental results should be performed accounting for both various geometries and material properties;
2) *Differentiation between modelling hypotheses*: the plausible modelling hypotheses able to simulate the response of RC structure by means of NLNAs should be involved in the calibration procedure. In fact, a comprehensive quantification of the resistance model uncertainties for NLNAs requires to account for the different modelling hypotheses which may be selected by engineers and practitioners;
3) *Probabilistic calibration*: in order to consider the differentiation between modelling hypotheses, it is necessary to define a probabilistic model able to represent the resistance model uncertainty random variable ϑ estimating the mean value μ_ϑ and the variance σ_ϑ^2. The treatment of the resistance model uncertainties can be developed following the Bayesian approach [37] as implemented in [12];
4) *Evaluation of the resistance model uncertainty safety factor* γ_{Rd}: grounding on the appropriate probabilistic model able to represent the resistance model uncertainty random variable ϑ, it is possible to estimate the partial safety factor γ_{Rd} as follows:

$$\gamma_{Rd} = \frac{1}{F^{-1}\left(\Phi\left(-\alpha_R \beta\right)\right)} \tag{4}$$

where $F(\vartheta)$ is the most likely cumulative probabilistic distribution function able to describe resistance model uncertainty random variable ϑ; Φ is the standard normal cumulative probabilistic distribution function; α_R is the first-order-reliability-method (FORM) sensitivity factor, assumed equal to 0.8 and 0.32 as suggested by [10] for dominant and non-dominant resistance variables, respectively; β is the reliability index [38].

In the next section, different experimental compressive tests performed on slender RC members are considered and reproduced through appropriate NLN models. These latter are defined considering different suitable and plausible modelling hypotheses in order to estimate the resistance model uncertainties and calibrate the corresponding values of the partial safety factor as described above. In this way, the results should cover the uncertainty deriving from a single options set taken by engineers and practitioners in line with their judgment and experience.

3. EXPERIMENTAL RESULTS AND NUMERICAL MODELS OF SLENDER REINFORCED CONCRETE COLUMNS

In this section, the results from the scientific literature related to the tests performed on slender RC columns are described and reproduced by means of appropriate NLN models. Firstly, an experimental database with 40 tests performed on RC columns having different slenderness, amount of reinforcement, material properties and test set configuration is collected. Then, the experimental results are numerically reproduced adopting nine different modelling hypotheses in order to investigate and characterize the resistance model uncertainty random variable ϑ.

3.1 Selection of experimental results from scientific literature

In this sub-section, the experimental tests performed on slender RC columns with outcomes known from the scientific literature are listed and described. The experimental database, herein considered, has been collected with the aim to account for tests with details as much as possible in line with the common practice for design and construction of RC structures. In particular, the selection has been carried out according to the limitations and specifications of widely recognized design Codes: EN1992 [36] and *fib* Model Code 2010 [10]. As discussed by [32], the experimental database for model uncertainty calibration should be defined within the field of application of the selected design Codes. In this investigation, EN1992 [36] and *fib* Model Code 2010 [10] frameworks are considered. According to [36] and [10], Table 1 summarizes the limitations concerning maximum and minimum provisions in terms of amount of longitudinal and transversal reinforcement. These limitations are herein adopted in order to select the experimental tests.

According to the mentioned above criteria, the literature references of [22]-[30] have been identified with the aim to collect the experimental database for the resistance model uncertainty investigation. In order to obtain the most likely estimation of the statistical parameters for the resistance modeling uncertainty random variable ϑ and, simultaneously, to respect the limitations of Table 1, a total number of short-term (without creep/shrinkage effects) 40 experimental results has been selected. The 40 outcomes from tests on slender RC columns have been selected between the results of the experimental campaigns of [22]-[30] in order to have a homogeneous representation of both geometrical and material properties, as described in the following.

Concerning the slenderness λ, a wide range of values between 15 and around 280 has been considered for the investigation. This choice has been performed in order to collect results concerning values of λ representative of common structural members as RC columns (e.g., λ around 15-30), of high RC bridge piers (e.g., λ from 30 to 90) and also of other extremely slender reinforced concrete members (with λ higher than 100). The experimental concrete compressive strength of the specimens, which can be identified as the related mean value [16], has been selected varying within the range 15-60 MPa as representative of normal concrete strength classes (i.e., ≤C50/60 [36]).

The experimental (i.e., mean) value of the yielding strength for reinforcement has been selected reflecting properties of steel according to grade 300, 400 and 500 MPa. The amount of reinforcement, both longitudinal and transversal, has been identified according to Table 1 with reinforcement ratio (i.e., total longitudinal reinforcement over concrete area) within the range 0.2-4%.

The main characteristics of the 40 experimental tests set [22]-[30] are reported in Table A1 and, in general, described in the Annex A. The static schemes related to the experimental tests of [22]-[30] can be distinguished in four different configurations denoted as *Type A*, *B*, *C* and *D* schemes, as depicted in Figure 1 and signed in Table A1.

3.2 Modelling hypotheses for non-linear numerical analysis of reinforced concrete columns

In this sub-section the different modelling hypotheses related to the definition of the numerical models of the 40 RC columns are described. The suitable and plausible modelling hypotheses are considered in order to cover the possible choices taken by engineers or practitioners. In fact, in compliance with [18]-[19], all the choices related to the definition of a NLN model affect significantly the prediction of the structural response. In detail, a specific modelling hypothesis affects the application of the basics principles of structural mechanics concerning materials constitutive relationships, kinematic compatibility and equilibrium between internal and external forces.

In this investigation, in line with the approach of [12], three widely diffused numerical codes used for non-linear analyses of RC buildings or structures combined to three assumptions concerning the tensile response of concrete are considered in order to differentiate the possible modelling hypotheses and reproduce the response of the 40 RC columns [22]-[30]. In this way, for each column, nine different structural models M_j *(j=1-9)* are defined as depicted in Figure 2. In detail, the software platforms ADINA [39], TNO DIANA [40] and OpenSees [41] have been selected with the aim to define the non-linear structural models. The mentioned above software codes will be denoted

anonymously within the paper as *Numerical code 1*, *2* and *3* in order to avoid favoritisms and/or negative advertisement to a specific software house. As described by [12], the use of a specific *Numerical code* in order to perform non-linear analyses of RC structures is one of the main sources of uncertainty of epistemic nature even if the analyst/designer is an expert in the field. The structural models M_j have been defined for the specimen in compliance to the experimental tests configurations (e.g., eccentricity) denoted as *Type A*, *B*, *C* and *D*, as depicted in Figure 1 in line to the descriptions reported by [22]-[30]. Note that as demonstrated in the experimental results, no any brittle failure due to shear force occurred. This outcome has also verified in all the numerical simulations.

According to each experimental test (as described in Table 1 and Figure 1), the main body of each column has been modelled by means of beam elements accounting for materials (i.e., concrete and steel reinforcement) and geometrical non-linearities. The edge and the mid-height enlargement of the cross sections have been modelled adopting beam elements with the assumption of linear-elastic behaviour for concrete (with Young modulus defined according to the experimental evidence). These assumptions, on one hand, allow to reduce the computational effort required for each simulation and, on the other hand, to concentrate all the non-linearities reproduced by the numerical models in the regions where they mostly develop within the specimens experimentally tested (in agreement to test descriptions provided by original authors). In addition, all the simulations have been performed according to the actual tests execution process. Firstly, the dead load has been applied to each column and then the experimental loading process [22]-[30] has been reproduced up to structural failure. The numerical simulations have been extended until the respect of the convergence criteria based on displacements (with tolerance set equal to 1%). The ultimate axial load has been defined as the axial load reached in correspondence of the last step before the loss of numerical convergence. Specifically, the *Type A* models present a statically determined scheme as showed in Figure 1(b). The *Type A* columns have been loaded along the centre of gravity of their cross-section, hence, the specimens are not subjected to a first order eccentricity of the axial force. In order to perform non-linear simulations through *Numerical codes 1*, *2* and *3*, it has been necessary to assign, after a calibration procedure, a minimum eccentricity value equal to 1/500 of the length of the column for all the *Type A* specimens to lead to a representative model able to provide results consistent with the experimental ones. From the physical point of view, this eccentricity may be representative of unavoidable imperfections (i.e., experimental uncertainty) related to the location of the point of application of the axial load during the experimental tests. In the case of the specimen 24D-2 of [23], the level of the restraint at the edges of the columns has been varied by the original authors in order to investigate its influence on the structural response. Then, in line with Figure 1(b), the *Type D* static scheme has been reproduced by means of a full restraint at the base and fixing the rotation and lateral displacement at the top of the column where the axial force is also applied (Figure 1(b) - *Type D*).

The columns realized with the *Type B* scheme present a statically determined configuration that, differently from the *Type A* specimens, has been realized introducing a first order eccentricity *e* where the axial load is applied as depicted in Fig. 1(a).

Regarding the *Type C* tests configurations, they presented a constant axial load applied in a first phase, and in a second phase, an incremental lateral load applied in the midspan of the column up to failure (Figure 1 (c)). The midspan stub element where the lateral load is applied has been modelled as a linear behaviour beam element. Concerning the *Type C* columns, no additional eccentricities have been defined in order to perform the simulation with *Numerical codes 1*, *2* and *3*.

Finally, the RC cross sections have been appropriately defined within *Numerical codes 1, 2* and *3* accounting for properties of the different materials distinguishing between concrete cover (i.e., un-confined concrete), concrete core (i.e., region influenced by confinement effect induced by shear reinforcements) and longitudinal ordinary reinforcements, as shown in Figure 1(d). Concerning the material constitutive relationships, the *Razvi-Saatcioglu* model [42] is assumed to reproduce the stress-strain response of concrete in compression with *Numerical codes 1, 2* and *3*. This model allows to take into account the distinction between un-confined and confined concrete behaviour.

The un-confined concrete compressive strength f_c is the one reported by the experimental references [22]-[30] for the 40 selected columns (Table A1). The deformation parameters and Young's modulus, if not reported by [22]-[30], are evaluated accordingly to [36] depending on the experimental values of the un-confined concrete compressive strength. The confined concrete compressive strength f_{cc} takes into account the contribution of transversal reinforcement and of the actual triaxial stress state of concrete within the core of the cross section. The variation of strength and ductility in compression, with respect to the un-confined configuration, are evaluated according to [42].
The response of concrete in tension has been object of differentiation in order to take into account the possible choices (i.e., epistemic uncertainty [12],[20]) that designers/analysts may perform with the aim to account for the fracture energy and the influence of the "tension stiffening effect". In compliance to the approach of [12], three possible responses have been considered: elastic-brittle, elastic with post peak linear tension softening (i.e., LTS) and elastic with perfectly plastic response after reaching the tensile concrete strength. The first and the third responses have been conceived as non-physical bounds of the possible representation of concrete tensile behaviour and so, they represent the epistemic uncertainty related to the material modelling [12]. The LTS model has been appropriately calibrated in line with [12] in order to fit the ultimate load obtained by the simulation with reference to the experimental one. This procedure has been performed for each experimental test and *Numerical code*. The Young modulus of concrete in tension has been assumed equal to the Young modulus in compression and has been evaluated together with the concrete tensile strength according to [36] (as, in general, no information are provided by the literature references [22]-[30]).
The constitutive model for the reinforcement steel has been characterized by a bi-linear elastic with hardening relationship. The yielding tensile strength f_y has been determined in compliance to [22]-[30] as shown in Table 1. The Young modulus, ultimate deformation and ultimate tensile strength have been identified accordingly to [22]-[30] if information is provided. Alternatively, a Young modulus set equal to 210 GPa, ultimate deformation set equal to 7.5% and ultimate tensile strength evaluated with 15% of hardening with respect to the reinforcement tensile yielding strength have been assumed also in line with [36].
In Table 2, the summary and the description of the modelling hypotheses performed within the *Numerical codes 1*, *2* and *3* are reported.

4. NON-LINEAR NUMERICAL ANALYSES OF SLENDER RC COLUMNS AND COMPARISON WITH THE EXPERIMENTAL RESULTS

In this Section, the results from the 360 non-linear simulations performed for the 40 RC columns of [22]-[30] are reported and commented. Table B1 reports and compares the outcomes in terms of maximum axial load R_{Mj} (j=1-9), reached through the non-linear simulations, to the associated experimental values R_{Exp} for each experimental test. The results are listed, for the different experimental investigations of [22]-[30] and also with reference to the different values of slenderness λ. Figure 3(b-j) reports the comparison, for each specimen, between R_{Model} and R_{Exp} differentiating between the 9 structural models M_j characterized by j=1-9 different modelling hypotheses, as described in Section 3. The realizations of the resistance random variable $\mathcal{9}$ for each structural model, evaluated in line with the approach of Section 2, are reported in Table B2 and shown in Figure 3(j) as a function of the slenderness λ. It can be recognized that the choice of a specific modelling hypothesis affects significantly the results of the numerical simulations in terms of ultimate axial load. In particular, the choice related to the selection of *Numerical Code* to reproduce the 40 experimental tests of [22]-[30] turns out to be the most relevant one.
Figure 3(a-i) and Tables B1-B2 show that the structural models $M_{1,2,3}$, $M_{4,5,6}$ and $M_{7,8,9}$ provide similar results when the model for the tensile response of concrete is varied according to Section 3. In particular, the choice of the tensile response of concrete does not affect significantly the results and, in detail, the use of an elastic-plastic response (i.e., $M_{3,6,9}$) leads to a slight overestimation of the ultimate axial load if compared to elastic-brittle and LTS material models.

It is also possible to observe how the effects due to the model uncertainty in terms of the mean value of ϑ are slightly lower for higher values of the eccentricity since an its increase leads to a more ductile mechanical behaviour before that the instability failure mode occurs, whereas, the dispersion of the data remains quite constant.

5. PROBABILISTIC ANALYSIS OF THE RESISTANCE MODEL UNCERTAINTY AND ESTIMATION OF THE PARTIAL SAFETY FACTOR

Next, the outcomes in terms of ratio $\vartheta = R_{Exp} / R_{Mj}$ reported in Section 4 represent the input data for the statistical and probabilistic analysis to estimate the partial safety factor γ_{Rd}, without any differentiation between the different "axial force-bending moment" interaction regimes. First of all, the most likely probabilistic model able to describe the resistance model uncertainty random variable is defined by means of an appropriate statistical inference procedure for the nine different modelling hypotheses. Hence, the Bayesian approach of [12] is adopted and extended with the aim to include also the scientific literature knowledge of [31] within the probabilistic calibration of the resistance model uncertainty random variable ϑ. Moreover, the potential influence of the experimental uncertainty on the estimation of statistical parameters for ϑ is also considered. Finally, the resistance model uncertainty partial safety factor γ_{Rd} is derived in line with the reliability differentiation of [10] for both new and existing RC structures.

5.1 Statistical inference and definition of the probabilistic model

This section reports the statistical characterization of the observed outcomes ϑ_i of the resistance model uncertainty random variable ϑ with the definition of the appropriate probabilistic model.
The statistical analysis has been performed with reference to the samples of the observations ϑ_i related to each set of the modelling hypotheses M_j with j=1-9 and to the associated updating information within the Bayes theory, as discussed in the next sub-section. The samples selected to define the updating information for each structural model M_j, in line with the approach of [12], are defined considering 320 of the 360 samples of the observations of ϑ_i with the exclusion of the themselves data (i.e., 40 observations ϑ_i) associated to the structural model itself M_j which is subjected to the Bayesian updating process [37]. The graphical representation of the ratios ϑ_i between R_{Exp} and R_{Mj} is reported in Fig.s 4 and 5 for the structural models M_3 and M_9, in sake of example. Fig.s 4(a,c) and 5(a,c) report the probability plots related the logarithm of the observations ϑ_i, proving the possibility to use the lognormal distribution in order to represent the resistance model uncertainty random variable ϑ. The Anderson-Darling statistical tests have been conducted, for each set of the modelling hypotheses M_j with j=1-9, confirming the validity of the hypothesis of lognormal probabilistic model with 5% significance levels. This result is also in line with [10] and [31]. The statistical parameters of the lognormal distributions (i.e., mean value μ_ϑ, standard deviation σ_ϑ and the related coefficient of variation $V_\vartheta = \sigma_\vartheta / \mu_\vartheta$), for the samples associated to each structural model M_j and the related updating information, are estimated by means of the maximum likelihood criteria (i.e., ML criteria) [43] and they represent the maximum likelihood estimators (i.e., MLEs). The relative frequency histograms and the associated lognormal probabilistic distributions are reported in Fig.s 4(b,d) and 5(b,d) for the structural models M_3 and M_9, as an example. In Tables 3 and 4 the MLEs associated to the prior and updating statistical parameters of the associated lognormal probabilistic distributions are reported. According to the ML criteria, by evaluating the inverse of the Fischer information matrices **C** [37], the variance of the statistical parameters μ_ϑ (i.e., C(1,1)) and σ_ϑ (i.e., C(2,2)), respectively, are also reported. Then, the most likely probabilistic model able to represent the samples of observations of ϑ_i is represented by the lognormal one and, in the following, it would be adopted in order to calibrate the resistance model uncertainty safety factor γ_{Rd}.

5.2 Bayesian updating to characterize the resistance modeling uncertainty random variable

The probabilistic treatment of the resistance modeling uncertainty random variable ϑ related to NLNAs of slender RC members is performed by means of a Bayesian approach [37] that allows to update the prior knowledge trough information deriving from further investigations or knowledge provided by different scientific sources. Specifically, the procedure adopted by [12] for the Bayesian updating and treatment of the resistance model uncertainty random variable is herein adopted.
When the scientific literature knowledge is considered for the Bayesian updating, we have referred to *JCSS Probabilistic Model Code 2001* [31]. In line with [31], the resistance modeling uncertainty random variable ϑ, related to buckling failure, can be modelled by means of a lognormal distribution having mean value μ_ϑ equal to 1.4 and coefficient of variation V_ϑ equal to 0.25. Note that the presence of the bias larger than unity, achieved in not recent investigations neglecting some positive effects in the resistance modelling (e.g., behaviour in tension for concrete, confinement effects), is however associated to a large value of the coefficient of variation. This information is almost in agreement with the estimates concerning the coefficient of variation V_ϑ derived in Sub-section 5.1 for the different prior and updating information (reported in Tables 3-4) and, it represents a "safe" overestimation of the actual value of V_ϑ. With reference to the mean value μ_ϑ, it can be observed that the estimates of Sub-section 5.1 lead to values (Tables 3-4) which are significantly lower if compared to the relevant "safe" bias μ_ϑ equal to 1.4 identified by [31]. In fact, the results in terms of μ_ϑ deriving from the different modeling hypotheses lead to values close to 1.00-1.10 and, in particular, for the structural models M_8 and M_9 a slightly "unsafe" bias (i.e., μ_ϑ below the unit) is observed as reported in Tables 3 and 4. This discrepancy suggests, in order to provide a comprehensive assessment of the random variable ϑ, to proceed with the probabilistic analysis proposed by [12] differentiating the Bayesian updating process between two different approaches denoted as *Approach A* and *Approach B*, which are schematically represented in Figure 6.
The *Approach A* is fully in line with the methodology adopted by [12] disregarding the scientific literature information of [31]. As previously introduced, the prior and updating data are represented, for each modelling hypothesis M_j with j=1-9, by the lognormal probabilistic distributions $f(\vartheta|M_j)$ (i.e., probability density function, PDF) or $F(\vartheta|M_j)$ (i.e., cumulative density function, CDF) and $f_{Mj}(\vartheta|z_j)$ or $F_{Mj}(\vartheta|z_j)$, respectively, with statistical parameter estimates reported in Table 3. The vector z_j groups the statistical parameters of the lognormal distributions associated to the updating information for each structural model M_j with j=1-9. The updating procedure using conjugate prior distribution is performed [37] and 9 different lognormal posterior distributions $f(\vartheta|M_j,z_j)$ - $F(\vartheta|M_j,z_j)$ conditional to the modeling hypotheses M_j with j=1-9 are evaluated and listed in Table 3 with the related statistical uncertainty represented by the variance of the mean μ_ϑ (i.e., C(1,1)) and of the standard deviation σ_ϑ (i.e., C(2,2)), respectively. Finally, the average posterior lognormal distribution $f(\vartheta|Z)$ - $F(\vartheta|Z)$ is derived averaging the statistical parameters of the 9 conditional posterior distributions, which are grouped in the vector Z. Table 3 reports the results of the *Approach A* procedure. In Figure 7, the graphical representation of the lognormal probabilistic distributions (i.e., PDFs in Figure 7(a) and CDFs in Figure 7(b)) is proposed.
The *Approach B* is conceived to include the scientific literature information of [31] within the Bayesian updating process of the *Approach A* [12]. For instance, the *Approach B* methodology is subdivided in 2 phases:

- in the *1st Phase*, the prior information is in line with the *Approach A* while, the updating information is represented for all the 9 modelling hypotheses M_j by a lognormal probabilistic distribution $f'(\vartheta) - F'(\vartheta)$ having mean value μ_ϑ equal to 1.4 and coefficient of variation V_ϑ equal to 0.25 in agreement with [31] and Table 4. Then, the nine *1st Phase* – conditional posterior lognormal distributions denoted as $f'(\vartheta|M_j) - F'(\vartheta|M_j)$ are evaluated according to the updating procedure using the conjugate prior distributions [37].

- in the *2nd Phase*, the updated prior information is represented by the nine *1st Phase* – conditional posterior lognormal distributions $f'(\vartheta|M_j) - F'(\vartheta|M_j)$ and the updating information is represented, in line with the *Approach A*, by the lognormal distributions $f_{Mj}(\vartheta|z_j) - F_{Mj}(\vartheta|z_j)$, with j=1-9. Finally, nine *2st Phase* – conditional posterior lognormal distributions $f'(\vartheta|M_j,z_j) - F'(\vartheta|M_j,z_j)$ are derived and the related statistical parameters are averaged to get the average posterior lognormal distribution $f'(\vartheta|Z') - F'(\vartheta|Z')$ (i.e., Z' vector of the average statistical parameters for the *Approach B*). Table 4 reports the results of the *Approach B* procedure.

Fig. 8 depicts the graphical representation of the lognormal probabilistic distributions (i.e., *1st Phase* PDFs in Figure 8(a) and CDFs in Figure 8(b); *2nd Phase* PDFs in Fig. 7(c) and CDFs in Fig. 7(d)).

5.3 Influence of the experimental uncertainty

In Sub-sections 5.1 and 5.2, the resistance model uncertainty random variable ϑ has been characterized considering the observed values of the ratios $\vartheta = R_{Exp}/R_{Mj}$ for each experimental test. As discussed by [44]-[46], the latter can be also affected by test or experimental uncertainties. The experimental uncertainty ε accounts for the uncertainties related to the tests procedures, accuracy of the tests methods, measurements errors (e.g., experimental value of the eccentricity), geometrical deviations of the specimens, loading and actual supports configuration. In order to appropriately address the statistical parameters related to the actual values of the resistance model uncertainty random variable ϑ, the influence of the experimental uncertainty ε (which can be assumed as a lognormal random variable with mean value μ_ε and coefficient of variation V_ε [21]) should be detached from the observed mean values μ_ϑ and coefficient of variation V_ϑ. In line with [45], well-calibrated tests methods on un-corroded RC members (as in the case of the tests of [22]-[30] herein adopted) may be considered as unbiased. Hence, the mean value μ_ε of the experimental uncertainty can be assumed, reasonably, set equal to 1.00. The coefficient of variation V_ε of the experimental uncertainty is particularly complicated to be evaluated and, [45] suggests to assume values ranging from 0.05 to 0.15 concerning tests on RC members in bending or compression. In this way, the actual values of the statistical parameters representing the resistance model uncertainty random variable ϑ can be derived in line with the following expressions [21], [44]-[46]:

$$\mu_{\vartheta,act} \approx \frac{\mu_\vartheta}{\mu_\varepsilon} \tag{5a}$$

$$V_{\vartheta,act} \approx \sqrt{V_\vartheta^2 - V_\varepsilon^2} \tag{5b}$$

where μ_ϑ and V_ϑ are the observed mean value and coefficient of variation, respectively, of the resistance model uncertainty random variable ϑ evaluated in line with the *Approach A* or *B* as described in Sub-section 5.2; μ_ε and V_ε are the mean value and coefficient of variation, respectively, of the experimental uncertainty ε; $\mu_{\vartheta.act}$ and $V_{\vartheta,act}$ are the actual mean value and coefficient of variation, respectively, of the resistance model uncertainty random variable ϑ deprived of the influence of the experimental uncertainty. As previously introduced, in case of unbiased tests on RC members, μ_ε is equal to 1.00, so, the actual mean value $\mu_{\vartheta.act}$ of the resistance model uncertainty ϑ converges to the observed mean value μ_ϑ. Concerning the characterization of the coefficient of variation V_ε associated to the experimental uncertainty, its quantification turns out to be complex. In particular, in case of compression tests on slender RC columns having small cross sections (around 150x150 mm), the influence of the geometrical imperfections (e.g., asymmetry of concrete properties due to casting procedures, misplacing of reinforcement and geometrical deviations) can be significantly higher if compared to RC members with larger dimensions [45].

Moreover, tests concerning extremely slender concrete columns may be strongly influenced by imperfections related to application of the loads and restraint configuration. For instance, in the following and also depicted in Fig. 6, two assumptions concerning the coefficient of variation V_ε are performed:

i. presence of a *limited* experimental uncertainty: V_ε may be considered as lower or equal to 0.05. In line with Eq.(5b) and the results of Table 3 and Table 4, this assumption leads to neglectable influence of experimental uncertainty and the actual value of the coefficient of variation $V_{\vartheta.act}$ which can be assumed as equal to the observed value V_ϑ;
ii. presence of a *significant* experimental uncertainty: V_ε is herein set equal to 0.10 (according to suggestions of [45],[46]). Eq.(5b) and results reported in Table 3 and Table 4 lead to an actual value of the $V_{\vartheta.act}$ which differs from the observed one V_ϑ.

Table 5 reports the actual statistical parameters (i.e., $\mu_{\vartheta.act}$ and $V_{\vartheta,act}$) for the lognormal probabilistic distributions able to represent the resistance model uncertainty random variable ϑ accounting for the influence of the experimental uncertainty ε. In case of a *significant* experimental uncertainty, with reference to both the *Approach A* and *B*, the actual values of coefficient of variation $V_{\vartheta,act}$ turn out to be smaller of around 10% if compared to the observed values V_ϑ. The lognormal probabilistic distributions (i.e., PDFs and CDFs) able to represent the resistance model uncertainty ϑ, in line with both the *Approach A* and *Approach B*, accounting for both *limited* and *significant* influence of the experimental uncertainty ε, are reported in Figure 9(a-b). In the following, the values of the statistics of Table 5 are used in order to derive the appropriate values of the model uncertainty safety factor γ_{Rd} to perform reliability assessment of slender RC members by means of NLNAs.

5.4 Evaluation of the partial safety factor

In the present sub-section, the estimation of the partial safety factor γ_{Rd} for resistance model uncertainty in non-linear numerical analyses of slender RC members is proposed in line with the safety formats [10]. The outcomes from the probabilistic assessment of the resistance model uncertainty random variable ϑ listed in Table 5 are considered. According to the assumptions of log-normal probabilistic model, the partial safety factor γ_{Rd} can be evaluated as follows [10],[12]:

$$\gamma_{Rd} = \frac{1}{\mu_{\vartheta,act}\exp\left(-\alpha_R \beta V_{\vartheta,act}\right)} \tag{6}$$

where $\mu_{\vartheta.act}$ and $V_{\vartheta,act}$ are the actual mean value and the coefficient of variation of the resistance model uncertainty random variable ϑ assumed according to Table 5 deprived of the influence of the geometrical uncertainty, respectively; α_R is the FORM sensitivity factor for resistance variables can be assumed equal to 0.32 and 0.8 [10],[38]-[35] accounting for the hypothesis of non-dominant and dominant variables, respectively; β is the target reliability index [38].

The partial safety factors γ_{Rd} evaluated with Eq. (6) are reported in Table 6 and Table 7 for the probabilistic calibration of resistance model uncertainty ϑ with *Approach A* and *Approach B*, respectively, performing the assumptions of both *limited* and *significant* level of experimental uncertainty. The target reliability indices β are assumed in agreement with the reliability differentiation of [10], distinguishing between structures of new realization and existing ones [15],[35],[31]. Moreover, the resistance model uncertainty random variable ϑ can be considered as dominant or non-dominant variable within the reliability analysis. According to [10], the modelling uncertainties random variables in general (i.e., both related to action and resistance models) may be assumed as non-dominant variables with less influence on the overall probability of failure with respect to the aleatory uncertainties which are related to random variability of material properties and actions. For instance, the value of the FORM factor α_R to derive the partial safety factors for the

modelling uncertainties is suggested to be set equal to 0.32. However, this assumption my lead to an underestimation of the influence of the resistance model uncertainty on the evaluation of structural reliability, in particular, when the coefficient of variation of ϑ turns out to be equal or higher than the coefficient of variation of the main involved aleatory random variables (e.g., concrete compressive strength with coefficient of variation set equal to 0.15 [10],[31]). As shown in Table 5, the coefficient of variations $V_{\vartheta,act}$ estimated with the *Approaches A* and *B* ranges between 0.15 and 0.22. This implies that the resistance model uncertainty random variable ϑ related to NLNAs of slender RC members may be assumed as dominant variable, with FORM factor α_R set equal to 0.8. Due to the mentioned above reasons, the derivation of the partial safety factor γ_{Rd} is performed in both the assumptions of non-dominant and dominant variable for the resistance modelling uncertainty ϑ. It can be noted that in case the resistance modelling uncertainty is considered as dominant variable, the aleatory uncertainties related to material properties may become non-dominant with significant reduction of the value of γ_R [12],[15].

Tables 6 and 7 report the values of the partial safety factors γ_{Rd} estimated with the *Approaches A* and *B*. The *Approach A*, which does not take into account the scientific literature information of [31], leads to values of γ_{Rd} slightly higher if compared to the ones descending from the *Approach B* even though the coefficient of variations $V_{\vartheta,act}$ of the *Approach A* are smaller in both the hypotheses of *limited* and *significant* influence of the experimental uncertainty (Table 5). The reason of this difference is related to the estimates of the bias (i.e., $\mu_{\vartheta.act}$) of the resistance model uncertainty random variable. In fact, the main consequence to consider the scientific literature information of [31], which is included in the calibration proposed by the *Approach B*, is to rise the mean value $\mu_{\vartheta.act}$ from 1.04 (i.e., nearly un-biased variable) obtained with the *Approach A* to the value of 1.13 (i.e., safely biased variable). However, this discrepancy in partially compensated by the estimated values of the coefficient of variation (which are higher for the *Approach B* with respect to the *Approach A*), leading to similar values of the estimated partial safety factors γ_{Rd}. Tables 6 and 7 report also partial safety factors suitable for the assessment of existing structures in line with the reliability differentiation proposed by [10]. However, most appropriate values of γ_{Rd} to be used for the assessment of existing slender RC structures may be achieved using Eq.(6) with statistical parameters defined by Table 5 and target reliability index β evaluated according to methodologies of [15].

Finally, grounding on the results of the present investigation and suggestions of [10], the partial safety factors γ_{Rd} accounting for the modelling uncertainty for NLNAs of slender RC members can be evaluated in line to the outcomes reported in Tables 6 and 7. In particular, concerning structures of new realization with moderate consequences of failure with 50 years of reference life, the partial safety factors γ_{Rd} can be set between 1.16-1.19 in line with the hypothesis of limited level of experimental uncertainty in benchmark test sets and between 1.12 -1.15 in the hypothesis of significant level of experimental uncertainty assuming ϑ as non-dominant random variable [10] within reliability analysis. However, the outcomes reported in Table 5 related to the coefficient of variation of resistance model uncertainty $V_{\vartheta,act}$ suggests that, concerning the non-linear numerical analysis of slender RC members, the resistance model uncertainty random variable may become a dominant variable within the reliability analysis (i.e., $V_{\vartheta,act}/V_C$ >1.0 and $V_{\vartheta,act}/V_S$ >1.0 where V_C and V_S are the coefficient of variation of concrete compressive strength and steel yielding strength random variables, generally, assumed as 0.15 and 0.05 [10] , respectively). In fact, in this case, always regarding new RC structures with moderate consequences of failure with 50 years of reference life, the partial safety factors γ_{Rd} can be set between 1.65-1.73 in line with the hypothesis of limited level of experimental uncertainty in benchmark test sets and between 1.50 -1.61 in the hypothesis of significant level of experimental uncertainty. Then, using the safety formats for non-linear numerical analyses of [3],[10],[34], the material properties random variables (i.e., aleatory uncertainties) can be considered as non-dominant with a significant reduction of the global factor γ_R that, in this assumption, turns out to be close to 1.00 in most of the cases.

The proposed partial safety factors are specific within the framework of the safety formats of [10] where the epistemic and aleatory uncertainties are treated separately through the adoption of the FORM sensitivity factors, as widely discussed. Alternatively, with reference to [47], the approach based on a "single global factor" can be adopted. In the latter, the both aleatory and epistemic sources of uncertainties are treated with a single global factor and the differentiation between dominant and non-dominant variables with the adoption of FORM sensitivity factors is not required. This last approach can be easily implemented in safety formats based on global factors as the "method of estimation of coefficient of variation (ECoV)" [10] and the "probabilistic method (PM)" [10]. In fact, as discussed in other investigations [12]-[13],[18],[48], the model uncertainty related to NLNAs is estimated on the basis of global structural response and properly fits the approach based on global factors. Although the "single global factor" approach can be considered advantageous with respect the framework of safety formats of [16], it is of difficult implementation in the case of the adoption of the "partial factor method (PFM)" [10]. In fact, the "PFM" requires the definition of a single NLNA characterized by the adoption of design values of material properties to account for the aleatory uncertainties (and then, not using the global factor γ_R). With the approach of the "PFM", the uncertainty associated to the definition of the NLN model should be accounted for by means of the model uncertainty factor γ_{Rd} that should be applied to global resistance [10],[16],[34]. For instance, the implementation of the "single global factor" approach within the "PFM" requires a rather deep discussion related to the possibility to use the statistical parameters of model uncertainty estimated on global response to determine material specific partial safety factors (i.e., γ_C for concrete compressive strength and γ_S for reinforcement yielding strength) including together both the aleatory and epistemic uncertainties. As the present study is referred to general application within all the different safety formats available from the literature [3],[10],[34], the results have been presented according to the framework of [10] that complies with the evaluation of separate global factors to account for aleatory and epistemic uncertainties.

6. CONCLUSIONS

The aim of the present investigation is related to the assessment of the epistemic uncertainty within global non-linear numerical analyses of slender reinforced concrete members. First of all, 40 experimental outcomes on reinforced concrete columns having slenderness ratio between 15 and 275 and different geometries in line with international codes limitations have been considered. The maximum experimental axial loads have been compared to the ones derived from appropriate NLNAs differentiated with nine modelling hypotheses in order to characterize the resistance model uncertainty random variable ϑ. The statistical assessment of the results leads to the conclusion that the most appropriate probabilistic model able to describe ϑ is the lognormal one. Then, two different approaches based on the Bayes theory, denoted as *Approach A* and *B*, have been adopted in order to perform the probabilistic analysis of the results. The *Approach A*, which does not take into account other literature information about the resistance model uncertainty of slender structural components, leads to the evaluation of the statistical parameters for lognormal probabilistic distribution set equal to 1.04 concerning the mean value μ_ϑ and to 0.18 concerning the coefficient of variation V_ϑ. The *Approach B* has been conceived to include within the probabilistic calibration also prior scientific literature information. So, the statistical parameters of resistance model uncertainty random variable ϑ as evaluated are μ_ϑ equal to 1.13 and V_ϑ equal to 0.22. Moreover, the influence of the experimental uncertainty on the estimation of μ_ϑ and V_ϑ has been investigated. In particular, in case of significant experimental uncertainty for the experimental tests considered for the resistance model uncertainty calibration, the actual coefficient of variation $V_{\vartheta,act}$ can be reduced by 10% with respect to the observed coefficient of variation V_ϑ. Finally, based on the results from probabilistic analysis of the resistance model uncertainty random variable ϑ, which quantifies the level of epistemic uncertainty, the partial safety factors γ_{Rd} in line with the global resistance format for NLNAs has been derived

differentiating between new and existing structures. Specifically, the partial safety factors γ_{Rd} in case of moderate consequences of failure of new structures with 50 years of reference life can be set between 1.16-1.19 (1.65-1.73) in line with the hypothesis of limited level of experimental uncertainty in benchmark test sets and between 1.12 -1.15 (1.50-1.61) in the hypothesis of significant level of experimental uncertainty assuming the random variable ϑ as non-dominant (dominant) within reliability analysis. The application of the partial safety factors γ_{Rd} so far evaluated, can be useful for design and assessment of RC slender members in structures or buildings within the global resistance format approach by means of refined non-linear numerical analyses.

ANNEX A: DESCRIPTION OF THE EXPERIMENTAL DATABASE

In the present Annex A, the summary of the experimental database adopted for the investigation of the epistemic uncertainty in NLNAs of slender RC members is reported and described.

The laboratory tests described by *Mehmel et al.* [22] refer to 16 slender RC columns. The experimental tests have been conducted with the *Type B* scheme (Figure 1(a)). In particular, 14 columns have been tested with the same eccentricity in both ends while, 2 columns presented different eccentricity values at the ends. Three different types of reinforcement were used and the cross-sections have been defined with three different sizes. For the present investigation, the columns 3.3, 5.1 and 4.1 have been selected as reported in Table A1.

The test campaign of *Saenz and Martin* [23] has been performed with 52 slender RC columns presenting rectangular cross section with different values of both reinforcement ratio and slenderness. The tests have been performed adopting *Type A* and *Type D* (Figure 1(b)) static schemes. The experimental results of specimens 24D-2 and 15D-2 have been considered in the present study (Table A1).

The investigation proposed by *Foster and Attard* [24] collects tests data related to 68 eccentrically loaded slender RC columns realized with both conventional and high-strength concrete. All the columns present the *Type B* static scheme (Fig. 1(a)) with square cross section of 150 x 150 mm and two different percentages of steel reinforcement ratios. For this work, the specimen 2L20-30, 2L20-60, 2L8-120R, 4L8-30, 4L20-120 and 4L8-120R have been considered (Table A1).

Pancholi [25] reports the outcomes of tests performed on 38 RC columns including also investigations about the creep effects (i.e., long-term loading). Those columns are characterized by high slenderness (i.e., λ greater than 200) and by two different dimensions of the square cross-section and two different reinforcement ratios. The loading process and tests arrangement are in compliance to the *Type A* configuration, as shown in Figure 1(b). Then, no eccentricity has been considered. For the current study and in compliance to Table A1, the columns without the creep effects and denoted as 5, 6, 17A, 20, 18, 8 and 7 have been selected.

The research of *Dracos* [26] included both short and long-term tests. The slenderness, the cross-section, the reinforcement ratio and the eccentricity vary between the experimental tests. All columns were simply supported according to the *Type A* and *Type B* test configurations (Figure 1(a-b)). Concerning the present investigation, the short-term S28, S30 and S25 tests columns have been considered (Table A1).

A wide experimental campaign counting a total number of 396 columns with rectangular and square cross sections has been reported by *Iwail et al.* [27]. The ratio of the column length to the minimum depth ranged from 6 to 26. Loads have been applied monotonically at each column end with the same eccentricities at both ends. The columns C000, C020, B020 and RL300 are herein considered, as described in Table A1, and present a static scheme in compliance to the *Type A* and *B* configurations (Figure 1(a-b)).

In *Chuang and Kong*'s investigation [28], 26 eccentrically loaded simply supported RC columns (*Type B* scheme – Figure 1(a)) have been experimentally tested. Both normal and high concrete compressive strength has been used. The cross-sections have been realized with two different sizes and three types of reinforcement and reinforcement ratio. According to Table A1, the columns A-17-0.25 and C-31.7-0.25 have been chosen.

The experimental program of *Barrera et al.* [29] reports the results of tests on 44 RC columns having rectangular cross-sections with variable dimensions. The length of the columns has been fixed equal to 3 m for all the specimens and these have been subjected first to the application of a constant axial load and then to a monotonic incremental lateral force applied in the midspan, according to the *Type C* scheme (Figure 1(c)), up to failure. The columns N30-10.5-C0-3-30 and H60-10.5-C0-1-30 have been selected (Table A1).

The laboratory tests of [30] have been realized subdividing the tests campaign in two series (i.e., pilot and main series). Both the series considered axially and eccentrically loaded slender RC columns. The pilot series consisted of 12 tests and the main series of 31 tests. The columns in the pilot series and in the first fifteen tests of the main series have been realized with the *Type A* and *B* (Figure 1(b)) simply supported tests schemes. In the other columns of the main series, the end conditions have been modified with a dubious characterization of the end degree of restraint, and, consequently these columns have been disregarded. The rectangular cross section varies between the tests. The columns III, Va, 2, I, VI ,15 ,3 ,8 ,9 ,12 and 6 have been considered in the present study, as shown in Table A1.

ANNEX B: RESULTS FROM NLNAs OF SLENDER RC COLUMNS AND OBSERVED VALUES FOR THE MODEL UNCERTAINTY

In this Annex B, Tables B1 and B2 report the outcomes of non-linear numerical simulations in terms of structural resistance (i.e., ultimate axial load) and the estimated outcomes for resistance uncertainty random variable ϑ.

NOTATION LIST

R_d	design value of global structural resistance;
F_d	design value of the actions;
R_{NLNA}	global structural resistance estimated by non-linear numerical analysis;
R_{Exp}	experimental value of the global structural resistance;
R_{Mj}	global structural resistance estimated by non-linear numerical analysis with reference to the j^{th} modelling hypothesis;
M_j	j^{th} modelling hypothesis to define the non-linear structural model with j=1-9;
x_{rep}	representative value of a geometric or material property;
γ_R	global resistance safety factor;
γ_{Rd}	resistance model uncertainty safety factor;
X	vector of basic variables included into the resistance model;
Y	vector of variables that may affect the resisting mechanism but are neglected in the resistance model;
α_R	first-order-reliability-method (FORM) sensitivity factor;
β	target value of the reliability index;
Φ	standard normal cumulative probabilistic distribution function;
ϑ	resistance model uncertainty random variable (observed);
ϑ_i	i^{th} realization of the resistance model uncertainty random variable (observed) with i=1-40;
μ_ϑ	mean value of the resistance model uncertainty random variable (observed);
σ_ϑ^2	variance of the resistance model uncertainty random variable (observed);
V_ϑ	coefficient of variation of the resistance model uncertainty random variable (observed);
ε	experimental uncertainty random variable;
μ_ε	mean value of the experimental uncertainty random variable;
V_ε	coefficient of variation of the experimental uncertainty random variable;
$\mu_{\vartheta,act}$	mean value of the resistance model uncertainty random variable deprived of the influence of the experimental uncertainty ε (actual);

$V_{\vartheta,act}$ coefficient of variation of the resistance model uncertainty random variable deprived of the influence of the experimental uncertainty ε (actual);

λ experimental value of the slenderness of the RC columns;

z_j vector which groups the statistical parameters of the lognormal distributions associated to the updating information for each structural model M_j with j=1-9;

Z vector of the average statistical parameters for the *Approach A*;

Z' vector of the average statistical parameters for the *Approach B;*

b experimental value of the base of the cross section of the RC columns (parallel to the axis around which flexure occur);

h experimental value of the height of the cross section of the RC columns (orthogonal to the axis around which flexure occur);

A_c experimental value of concrete area of the cross section of the RC columns;

L_{tot} experimental value of total length of the RC columns;

L experimental value of length of the main body of the RC columns;

Φ_l diameter of the main longitudinal reinforcement bars;

Φ_w diameter of the shear reinforcement bars;

A_{sl} total area of the main longitudinal reinforcement bars;

ρ_l longitudinal geometrical reinforcement ratio;

s longitudinal spacing between shear reinforcements;

e experimental value of the eccentricity adopted to apply the axial load on the RC columns.

f_c experimental value of the cylinder concrete compressive strength;

f_y experimental value of the reinforcement tensile yielding strength;

REFERENCES

[1] *fib* Bulletin N°45: Practitioner's guide to finite element modelling of reinforced concrete structures – State of the art report, Lausanne, 2008.

[2] NIST GCR 17-917-46v3. Guidelines for Nonlinear Structural Analysis for Design of Buildings, U.S. Department of Commerce, Engineering Laboratory National Institute of Standards and Technology, Gaithersburg, USA, 2017.

[3] Shlune H, Gylltoft K, Plos M. Safety format for non-linear analysis of concrete structures. Magazine of Concrete Research 2012; 64(7): 563-574.

[4] Holicky, M. (2006) Global resistance factor reinforced concrete members, ACTA POLITECHNICA, CTU, Prague, 2006.

[5] Sykora M., Holicky M., Safety Format for Non-linear Analysis in the Model Code –Verification of Reliability Level. Proceeding of fib Symposium on Concrete Engineering for excellence and efficiency, Prague, Czech Concrete Society, 2011 – p.p. 943-946.

[6] Cervenka V., Global safety formats in fib Model Code 2010 for design of concrete structures, Proceedings of the 11th Probabilistic Workshop, Brno, 2013.

[7] Valašík A, Benko V and Täubling B: Reliability assessment of slender concrete columns at the stability failure, AIP Conference Proceedings 1922, 130010 (2018); https://doi.org/10.1063/1.5019140.

[8] Mohamed A, Soares R and Venturini WS: Partial safety factors for homogeneous reliability of nonlinear reinforced concrete columns, Structural Safety, 23, pp.137-156, 2001.

[9] Campione G, Cavaleri L, Di Trapani F and Ferrotto MF: Frictional Effects in Structural Behavior of No-End-Connected Steel-Jacketed RC Columns: Experimental Results and New Approaches to Model Numerical and Analytical Response, Journal of Structural Engineering (ASCE), 143(8), 2017, 10.1061/(ASCE)ST.1943-541X.0001796

[10] *fib* Model Code for Concrete Structures 2010. *fib* 2013. Lausanne.

[11] Cervenka V., Reliability –based non-linear analysis according to fib Model Code 2010, Structures Concrete, Journalof the fib, vol. 14, March 2013, ISSN1464-4177, p.p.19-28, 2011.

[12] P. Castaldo, D. Gino, G. Bertagnoli, G. Mancini (2018): Partial safety factor for resistance model uncertainties in 2D non-linear analysis of reinforced concrete structures, Engineering Structures, 176, 746-762. https://doi.org/10.1016/j.engstruct.2018.09.041.

[13] P. Castaldo, D. Gino, G. Bertagnoli, G. Mancini (2020): Resistance model uncertainty in non-linear finite element analyses of cyclically loaded reinforced concrete systems, Engineering Structures, 211(2020), 110496, https://doi.org/10.1016/j.engstruct.2020.110496

[14] ISO 2394. General principles on reliability for structures. Genéve. 1998.

[15] *fib* Bulletin N°80. Partial factor methods for existing concrete structures, Lausanne, Switzerland; 2016.

[16] P. Castaldo, D. Gino, G. Mancini (2019): Safety formats for non-linear analysis of reinforced concrete structures: discussion, comparison and proposals, Engineering Structures, 193, 136-153, https://doi.org/10.1016/j.engstruct.2018.09.041.

[17] Blomfors M., Engen M. and Plos M. : Evaluation of safety formats for non-linear Finite Element Analyses of statically indeterminate concrete structures subjected to different load paths, Structural Concrete, 17(1), pp. 44-51, 2016, 10.1002/suco.201500059

[18] Engen M, Hendriks MAN, Köhler J, Øverli JA, Åldtstedt E. A quantification of modelling uncertainty for non-linear finite element analysis of large concrete structures. Structural Safety 2017; 64: 1-8.

[19] Gino D, Bertagnoli G, La Mazza D, Mancini G. A quantification of model uncertainties in NLFEA of R.C. shear walls subjected to repeated loading, Ingegneria Sismica, Anno XXXIV Special Issue, pp. 79-91, 2017.

[20] Kiureghian AD, Ditlevsen O. Aleatory or epistemic? Does it matter?. Structural Safety, 31:105-112, 2009.

[21] Holický M, Retief JV, Sikora M. Assessment of model uncertainties for structural resistance. Probabilistic Engineering Mechanics 2016; 45: 188-197.
[22] A Mehmel, H Schwarz, KH Karperek, and J Makovi. Tragverhalten ausmittig beanspruchter stahlbetondruckglieder. institut für baustatik, eht, deutscherausschuss für stahlbeton, heft 204, 1969.
[23] Luis P Saenz and Ignacio Martin. Test of reinforced concrete columns with high slenderness ratios. In Journal Proceedings, volume 60, pages 589–616, 1963.
[24] Stephen J Foster and Mario M Attard. Experimental tests on eccentrically loaded high strength concrete columns. Structural Journal, 94(3):295–303, 1997.
[25] VR Pancholi. The Instability of Slender Reinforced Concrete Columns. PhD thesis, University of Bradford, 1977.
[26] Adriana Dracos. Long slender reinforced concrete columns. PhD thesis, University of Bradford, 1982.
[27] S.IwaiI, K. Minami, and M. Wakabayashi. Stability of slender reinforced concrete columns subjected to biaxially eccentric loads, 1986.
[28] PH Chuang and FK Kong. Large-scale tests on slender, reinforced concrete columns. Structural Engineer, 75(23):410–16, 1997.
[29] AC Barrera, JL Bonet, Manuel L Romero, and PF Miguel. Experimental tests of slender reinforced concrete columns under combined axial load and lateral force. Engineering Structures, 33(12):3676–3689, 2011.
[30] Oskar Baumann. Die Knickung der Eisenbeton-Säulen. PhD thesis, ETH Zurich, 1935.
[31] JCSS. JCSS Probabilistic Model Code. 2001.
[32] Castaldo P, Gino D, Carbone VI, Mancini G. Framework for definition of design formulations from empirical and semi-empirical resistance models, Structural Concrete, 1–8, 2018.
[33] CEN. EN 1990: Eurocode – Basis of structural design. CEN 2013. Brussels.
[34] Allaix DL, Carbone VI, Mancini G. Global safety format for non-linear analysis of reinforced concrete structures. Structural Concrete 2013; 14(1): 29-42.
[35] ISO 2394. General principles on reliability for structures. Genéve. 2015.
[36] CEN. EN 1992-1-1: Eurocode 2 – Design of concrete structures. Part 1-1: general rules and rules for buildings. CEN 2014. Brussels.
[37] Gelman A, Carlin JB, Stern HS, Dunson DB, Vehtari A, Rubin DB. Bayesian data analysis. 3rd ed. CRC Press; 2014.
[38] Hasofer AM, Lind NC. Exact and invariant second moment code format, Journal of the Engineering Division ASCE 1974; 100(EM1): 111-121.
[39] ADINA R & D. Inc.. 71 Elton Avenue Watertown. MA 02472. USA. 2014.
[40] DIANA FEA BV. Delftechpark 19a 2628 XJ Delft. The Netherlands. 2017.
[41] F. McKenna, G.L. Fenves, M.H. Scott, Open system for earthquake engineering simulation, University of California, Berkeley, CA, 2000.
[42] Murat Saatcioglu and Salim R Razvi. Strength and ductility of confined concrete. Journal of Structural engineering, 118(6):1590–1607, 1992.
[43] Faber, Michael Havbro Statistics and Probability Theory, Springer, 2012.
[44] Sykora M, Holicky M (2013) Assessment of uncertainties in mechanical models. AMM 378:13–18.
[45] M. Sykora, M.Holicky, M.Prieto ,P.Tanner, Uncertainties in resistance models for sound and corrosion-damaged RC structures according to EN1992-1-1, Mater. Struct. 48(2014) 3415–3430.
[46] Ellingwood BR, Galambos TV, MacGregor JG, Cornell CA (1980) Development of a probability based load criterion for American national standard A58: building code 3428 Materials and Structures (2015) 48:3415–3430.
[47] Moccia F, Yu Q, Fernández Ruiz M, Muttoni A. Concrete compressive strength: From material characterization to a structural value. Structural Concrete. 2020;1–21.

[48] Cervenka V, Cervenka J and Kadlek L (2018) Model uncertainties in numerical simulations of reinforced concrete structures, Structural Concrete, 2018;19:2004–2016.

TABLES

Table 1. Criteria for selection of experimental results according to EN1992 [36] and to *fib* Model Code 2010 [10] limitations for reinforcement.

Type of reinforcement	**Detail**	**Limitation***
Longitudinal reinforcement	Minimum diameter $\Phi_{l,min}$ [mm]	8
	Minimum reinforcement area $A_{sl,min}$ [mm^2]	$0.002 \cdot A_c$ *(with $A_c = b \cdot h$)*
	Maximum reinforcement area $A_{sl,max}$ [mm^2]	$0.04 \cdot A_c$
Transversal reinforcement	Minimum diameter $\Phi_{w,min}$ [mm]	$\max(0.25 \cdot \Phi_l; 6\text{ mm})$
	Maximum spacing s_{max} [mm]	$\min(20 \cdot \Phi_l; b; h; 400\text{ mm})$
	Further dispositions	- Every longitudinal bar in a corner should be held by transverse reinforcement - No bar within a compression zone shall be at a distance greater than 150 mm from a restrained bar

*suggested values

Table 2. Modelling hypotheses for the non-linear simulations of the 40 RC columns by [22]-[30].

	Numerical code 1	**Numerical code 2**	**Numerical code 3**
Equilibrium of forces	- Solution of non-linear system of equations: full Newton-Raphson iterative method; - Equilibrium evaluated in each iteration with reference to the deformed configuration accounting for the second order effects; maximum number of iterations for each load step: 100; - Convergence criteria based on displacements (with tolerance set equal to 1%); - Sizes of the incremental load steps defined with reference to experiments execution and iterative procedure in order achieve numerical accuracy;		
Kinematic compatibility	- 2 nodes beam elements selected according to the finite elements available from each *Numerical code* library [39],[40] (force-based approach for fiber beams elements [41]); - Element size defined in line with an iterative process accounting for the numerical accuracy;		
Constitutive relationships	*Concrete:* - Mono-axial non-linear model for un-confined and confined concrete in compression defined according to [42]; - Tensile response of concrete reproduced by means 3 different hypotheses: 1) Elastic – Brittle (i.e., brittle); 2) Elastic with post peak linear tension softening (i.e., LTS); 3) Elastic – perfectly plastic (i.e., plastic); *Reinforcements:* - Bi-linear elastic – plastic with hardening; The values of material properties (i.e., strengths, Young's modulus, ultimate strains, etc.) have been defined in line with the data provided by the original research papers [22]-[30] and in compliance to [36] if missing.		

Table 3. Statistical parameters (i.e., mean values and coefficients of variation) of the prior, posterior and new information distribution functions with related statistical uncertainty concerning the *Approach A*.

Structural Model	*Prior distributions (Lognormal)* $F(\vartheta \mid M_j)$		*Statistical uncertainty*		*Updating information (Lognormal)* $F_{Mj}(\vartheta \mid z_j)$		*Statistical uncertainty*		*Conditional posterior distributions (Lognormal)* $F(\vartheta \mid M_j, z_j)$		*Statistical uncertainty*	
	μ_ϑ [-]	V_ϑ [-]	*C(1,1)*	*C(2,2)*	μ_ϑ [-]	V_ϑ [-]	*C(1,1)*	*C(2,2)*	μ_ϑ [-]	V_ϑ [-]	*C(1,1)*	*C(2,2)*
1	1.05	0.21	$1.05 \cdot 10^{-3}$	$5.43 \cdot 10^{-4}$	1.04	0.18	$9.70 \cdot 10^{-5}$	$4.87 \cdot 10^{-5}$	1.05	0.19	$3.68 \cdot 10^{-4}$	$2.85 \cdot 10^{-4}$
2	1.02	0.19	$8.83 \cdot 10^{-4}$	$4.59 \cdot 10^{-4}$	1.05	0.18	$9.93 \cdot 10^{-5}$	$4.99 \cdot 10^{-5}$	1.04	0.18	$3.41 \cdot 10^{-4}$	$2.44 \cdot 10^{-4}$
3	1.01	0.20	$1.03 \cdot 10^{-3}$	$5.33 \cdot 10^{-4}$	1.05	0.18	$9.67 \cdot 10^{-5}$	$4.86 \cdot 10^{-5}$	1.03	0.19	$3.68 \cdot 10^{-4}$	$2.86 \cdot 10^{-4}$
4	1.17	0.20	$9.73 \cdot 10^{-4}$	$5.06 \cdot 10^{-4}$	1.03	0.17	$9.30 \cdot 10^{-5}$	$4.67 \cdot 10^{-5}$	1.10	0.20	$3.85 \cdot 10^{-4}$	$3.12 \cdot 10^{-4}$
5	1.10	0.17	$7.22 \cdot 10^{-4}$	$3.75 \cdot 10^{-4}$	1.04	0.18	$1.01 \cdot 10^{-4}$	$5.05 \cdot 10^{-5}$	1.07	0.18	$3.19 \cdot 10^{-4}$	$2.15 \cdot 10^{-4}$
6	1.10	0.20	$9.85 \cdot 10^{-4}$	$5.12 \cdot 10^{-4}$	1.04	0.18	$9.69 \cdot 10^{-5}$	$4.87 \cdot 10^{-5}$	1.07	0.19	$3.63 \cdot 10^{-4}$	$2.78 \cdot 10^{-4}$
7	1.01	0.12	$3.45 \cdot 10^{-4}$	$1.79 \cdot 10^{-4}$	1.05	0.19	$1.07 \cdot 10^{-4}$	$5.39 \cdot 10^{-5}$	1.03	0.16	$2.46 \cdot 10^{-4}$	$1.27 \cdot 10^{-4}$
8	0.99	0.09	$2.11 \cdot 10^{-4}$	$1.10 \cdot 10^{-4}$	1.05	0.19	$1.09 \cdot 10^{-4}$	$5.47 \cdot 10^{-5}$	1.02	0.15	$2.25 \cdot 10^{-4}$	$1.07 \cdot 10^{-4}$
9	0.96	0.14	$4.71 \cdot 10^{-4}$	$2.45 \cdot 10^{-4}$	1.06	0.18	$1.03 \cdot 10^{-4}$	$5.17 \cdot 10^{-5}$	1.01	0.17	$2.83 \cdot 10^{-4}$	$1.69 \cdot 10^{-4}$

	Average posterior distribution (Lognormal) $F(\vartheta \mid Z)$	
Average statistical parameters	μ_ϑ [-]	V_ϑ [-]
	1.04	0.18

Table 4. Statistical parameters (i.e., mean values and coefficients of variation) of the prior, posterior and new information distribution functions with related statistical uncertainty concerning the *Approach B.*

Structural Model	**1st Phase**											
	Prior distributions (Lognormal) $F(\vartheta \mid M_j)$		*Statistical uncertainty*		*Scientific literature information (Lognormal)* $F'(\vartheta)$		*Statistical uncertainty*		*Conditional posterior distributions (Lognormal)* $F'(\vartheta \mid M_j)$		*Statistical uncertainty*	
	μ_ϑ [-]	V_ϑ [-]	*C(1,1)*	*C(2,2)*	μ_ϑ [-]	V_ϑ [-]	*C(1,1)*	*C(2,2)*	μ_ϑ [-]	V_ϑ [-]	*C(1,1)*	*C(2,2)*
1	1.05	0.21	$1.05 \cdot 10^{-3}$	$5.43 \cdot 10^{-4}$					1.22	0.24	$5.94 \cdot 10^{-3}$	$7.44 \cdot 10^{-4}$
2	1.02	0.19	$8.83 \cdot 10^{-4}$	$4.59 \cdot 10^{-4}$					1.21	0.24	$5.92 \cdot 10^{-3}$	$7.37 \cdot 10^{-4}$
3	1.01	0.20	$1.03 \cdot 10^{-3}$	$5.33 \cdot 10^{-4}$					1.21	0.26	$6.49 \cdot 10^{-3}$	$8.87 \cdot 10^{-4}$
4	1.17	0.20	$9.73 \cdot 10^{-4}$	$5.06 \cdot 10^{-4}$					1.28	0.21	$4.45 \cdot 10^{-3}$	$4.16 \cdot 10^{-4}$
5	1.10	0.17	$7.22 \cdot 10^{-4}$	$3.75 \cdot 10^{-4}$	1.40 [31]	0.25 [31]	-	-	1.25	0.21	$4.48 \cdot 10^{-3}$	$4.23 \cdot 10^{-4}$
6	1.10	0.20	$9.85 \cdot 10^{-4}$	$5.12 \cdot 10^{-4}$					1.25	0.23	$5.12 \cdot 10^{-3}$	$5.52 \cdot 10^{-4}$
7	1.01	0.12	$3.45 \cdot 10^{-4}$	$1.79 \cdot 10^{-4}$					1.20	0.22	$4.97 \cdot 10^{-3}$	$5.19 \cdot 10^{-4}$
8	0.99	0.09	$2.11 \cdot 10^{-4}$	$1.10 \cdot 10^{-4}$					1.19	0.22	$4.95 \cdot 10^{-3}$	$5.17 \cdot 10^{-4}$
9	0.96	0.14	$4.71 \cdot 10^{-4}$	$2.45 \cdot 10^{-4}$					1.18	0.25	$6.17 \cdot 10^{-3}$	$8.01 \cdot 10^{-4}$

Structural Model	**2nd Phase**											
	Updated prior distributions (Lognormal) $F'(\vartheta \mid M_j)$		*Statistical uncertainty*		*Updating information (Lognormal)* $F_{Mj}(\vartheta \mid z_j)$		*Statistical uncertainty*		*Posterior distributions (Lognormal)* $F'(\vartheta \mid M_j, z_j)$		*Statistical uncertainty*	
	μ_ϑ [-]	V_ϑ [-]	*C(1,1)*	*C(2,2)*	μ_ϑ [-]	V_ϑ [-]	*C(1,1)*	*C(2,2)*	μ_ϑ [-]	V_ϑ [-]	*C(1,1)*	*C(2,2)*
1	1.22	0.24	$5.94 \cdot 10^{-3}$	$7.44 \cdot 10^{-4}$	1.04	0.18	$9.70 \cdot 10^{-5}$	$4.87 \cdot 10^{-5}$	1.13	0.23	$5.06 \cdot 10^{-4}$	$5.39 \cdot 10^{-4}$
2	1.21	0.24	$5.92 \cdot 10^{-3}$	$7.37 \cdot 10^{-4}$	1.05	0.18	$9.93 \cdot 10^{-5}$	$4.99 \cdot 10^{-5}$	1.13	0.22	$5.00 \cdot 10^{-4}$	$5.26 \cdot 10^{-4}$
3	1.21	0.26	$6.49 \cdot 10^{-3}$	$8.87 \cdot 10^{-4}$	1.05	0.18	$9.67 \cdot 10^{-5}$	$4.86 \cdot 10^{-5}$	1.13	0.23	$5.17 \cdot 10^{-4}$	$5.62 \cdot 10^{-4}$
4	1.28	0.21	$4.45 \cdot 10^{-3}$	$4.16 \cdot 10^{-4}$	1.03	0.17	$9.30 \cdot 10^{-5}$	$4.67 \cdot 10^{-5}$	1.16	0.22	$4.89 \cdot 10^{-4}$	$5.02 \cdot 10^{-4}$
5	1.25	0.21	$4.48 \cdot 10^{-3}$	$4.23 \cdot 10^{-4}$	1.04	0.18	$1.01 \cdot 10^{-4}$	$5.05 \cdot 10^{-5}$	1.14	0.22	$4.71 \cdot 10^{-4}$	$4.66 \cdot 10^{-4}$
6	1.25	0.23	$5.12 \cdot 10^{-3}$	$5.52 \cdot 10^{-4}$	1.04	0.18	$9.69 \cdot 10^{-5}$	$4.87 \cdot 10^{-5}$	1.14	0.22	$4.91 \cdot 10^{-4}$	$5.08 \cdot 10^{-4}$
7	1.20	0.22	$4.97 \cdot 10^{-3}$	$5.19 \cdot 10^{-4}$	1.05	0.19	$1.07 \cdot 10^{-4}$	$5.39 \cdot 10^{-5}$	1.12	0.22	$4.62 \cdot 10^{-4}$	$4.50 \cdot 10^{-4}$
8	1.19	0.22	$4.95 \cdot 10^{-3}$	$5.17 \cdot 10^{-4}$	1.05	0.19	$1.09 \cdot 10^{-4}$	$5.47 \cdot 10^{-5}$	1.12	0.21	$4.58 \cdot 10^{-4}$	$5.42 \cdot 10^{-4}$
9	1.18	0.25	$6.17 \cdot 10^{-3}$	$8.01 \cdot 10^{-4}$	1.06	0.18	$1.03 \cdot 10^{-4}$	$5.17 \cdot 10^{-5}$	1.12	0.22	$4.95 \cdot 10^{-4}$	$5.16 \cdot 10^{-4}$

Average statistical parameters	*Posterior distribution (Lognormal)* $F'(\vartheta \mid Z')$	
	μ_ϑ [-]	V_ϑ [-]
	1.13	0.22

Table 5. Statistical parameters (i.e., mean values and coefficients of variation) accounting for the influence of the level of experimental uncertainty concerning the *Approaches A* and *B*.

Approach	**Experimental uncertainty ε**	**Actual statistical parameters for resistance model uncertainty random variable ϑ**	
		$\mu_{\vartheta,act}$ [-]	$V_{\vartheta,act}$ [-]
A	*Limited* $V_\varepsilon \leq 0.05$	1.04	0.18
	Significant $V_\varepsilon = 0.10$		0.15
B	*Limited* $V_\varepsilon \leq 0.05$	1.13	0.22
	Significant $V_\varepsilon = 0.10$		0.20

Table 6. Partial safety factors γ_{Rd} for plane stress NLNAs of slender RC structures in the hypothesis of dominant resistance variable depending on the target reliability level [10] - *Approach A*.

	Reference life	**Consequences of failure**	**Reliability index β**	**FORM factor α_R**	**Partial safety factor γ_{Rd}**	
					Experimental uncertainty	
					Limited	*Significant*
New structures	[Years]	[-]	[-]	[-]	[-]	[-]
	50	Low	3.1	Non-dominant 0.32	*1.14*	*1.11*
		Moderate	3.8		*1.19*	*1.15*
		High	4.3		*1.22*	*1.17*
		Low	3.1	Dominant 0.8	*1.49*	*1.38*
		Moderate	3.8		*1.65*	*1.50*
		High	4.3		*1.77*	*1.59*
	Reference life		**Reliability index β**	**FORM factor α_R**	**Partial safety factor γ_{Rd}**	
					Experimental uncertainty	
					Limited	*Significant*
Existing structures	[Years]		[-]	[-]	[-]	[-]
	50		3.1 - 3.8	Non-dominant 0.32	*1.14-1.19*	*1.11-1.15*
	15		3.4 - 4.1		*1.16-1.21*	*1.13-1.16*
	1		4.1 - 4.7		*1.21-1.25*	*1.16-1.20*
	50		3.1 - 3.8	Dominant 0.8	*1.49-1.65*	*1.38-1.50*
	15		3.4 - 4.1		*1.56-1.72*	*1.43-1.56*
	1		4.1 - 4.7		*1.72-1.87*	*1.56-1.67*

Table 7. Partial safety factors γ_{Rd} for plane stress NLNAs of slender RC structures in the hypothesis of dominant resistance variable depending on the target reliability level [10] - *Approach B.*

	Reference life	**Consequences of failure**	**Reliability index β**	**FORM factor α_R**	**Partial safety factor γ_{Rd}**	
					Experimental uncertainty	
					Limited	*Significant*
New structures	[Years]	[-]	[-]	[-]	[-]	[-]
	50	Low	3.1	Non-dominant 0.32	*1.10*	*1.07*
		Moderate	3.8		*1.16*	*1.12*
		High	4.3		*1.20*	*1.16*
		Low	3.1	Dominant 0.8	*1.53*	*1.44*
		Moderate	3.8		*1.73*	*1.61*
		High	4.3		*1.89*	*1.74*
	Reference life		**Reliability index β**	**FORM factor α_R**	**Partial safety factor γ_{Rd}**	
					Experimental uncertainty	
					Limited	*Significant*
Existing structures	[Years]		[-]	[-]	[-]	[-]
	50		3.1 - 3.8	Non-dominant 0.32	*1.10-1.16*	*1.07-1.12*
	15		3.4 - 4.1		*1.12-1.18*	*1.09-1.14*
	1		4.1 - 4.7		*1.18-1.23*	*1.14-1.19*
	50		3.1 - 3.8	Dominant 0.8	*1.53-1.73*	*1.44-1.73*
	15		3.4 - 4.1		*1.61-1.82*	*1.51-1.69*
	1		4.1 - 4.7		*1.82-2.03*	*1.69-1.85*

Table A1. Experimental database collected for the investigation.

Ref. [*]	**Exp. test**	**Type**	L_{tot} **[mm]**	L **[mm]**	b **[mm]**	h **[mm]**	λ **[-]**	f_c **[MPa]**	f_y **[MPa]**	$\rho_l=A_{sl}/A_C$ **[%]**	e/h **[mm]**	$R_{Exp,i}$ **[kN]**
[24]	2L20-30	*B*	1450	650	150	150	15	40.0	480.0	2.0	0.133	750.0
	2L20-60							43.0			0.133	700.0
	2L8-120R							56.0		4.1	0.053	1092.0
	4L8-30							43.0			0.053	1100.0
	4L20-120							40.0			0.133	900.0
	4L8-120R							56.0			0.053	1247.0
[27]	C000	*A*	680	600	120	120	17	27.0	347.2	4.0	-	559.6
	C020	*B*									0.200	327.3
	B020		1880	1800			52	27.6	355.0		0.200	271.5
	RL300		3000	2920	120	180	56	31.0	360.9	2.6	0.167	474.3
[28]	A-17-0.25	*B*	3400	2800	300	200	48	38.2	493.0	3.3	0.250	1181.4
	C-31.7-0.25		3800	3260	200	120	94	44.4	520.0	3.4		333.4
[22]	3.3	*B*	3400	2700	254	159	59	35.3	509.9	1.1	0.082	782.6
	5.1							40.6	426.8	3.1	0.165	735.5
	4.1		4500	3800	253	150	88	40.5	509.9	1.2	0.163	367.7
[29]	N30-10.5-C0-3-30	*C*	3300	2940	140	150	68	29.5	538.0	3.2	-	16.6 (280)[*1]
	H60-10.5-C0-1-30							58.5	531.0	1.4		17.2 (412)[*1]
[30]	III	*A*	3210	3000	140	140	74	16.1	294.2	1.4	-	343.2
	Va		3240		178	140		26.4	281.8	1.6		684.5
	2		3230	3010	250	125	83	33.5	304.0	0.6		235.4
	I		3210	3000	200	100	104	15.2	294.2	1.6		264.8
	VI		3000		198	98	106	24.9	294.2			392.3
	15		6510	6310	247	161	136	33.0	294.2	0.8		549.2
	3				250	160	137	33.5	294.2			666.9
	8		3230	3010	250	126	83	20.4	304.0	0.6	0.200	235.4
	9	*B*	6510	6310	250	162	135	24.5	294.2	0.8		205.9
	12							29.7	294.2		0.300	112.8
	6				250	160	137	32.2	294.2		0.200	225.6
[23]	24D-2	*D*	2697	2697	127	90	104	20.8	247.5	2.5	-	198.4
	15E-2	*A*	3597	3597			139	20.1	247.5			161.0
[26]	S28	*B*	5000	5000	104	104	167	24.4	304.0	4.2	0.144	44.0
	S30							25.7	300.0			48.0
	S25		6000	6000			200	24.7	282.0			36.0
[25]	5	*A*	6004	6004	100	100	208	33.1	278.5	4.5	-	72.7
	6							35.6				72.2
	17A		4940	4940	76	76	225	25.8	300.4	5.4		31.9
	20		5327	5327			243	38.1				37.9
	18							38.2				33.9
	8		6004	6004			274	36.5				31.9
	7							39.3				29.9

(-)*[1] Constant value of axial load applied to the column during the experimental test.

Note: The slenderness of the RC columns, having rectangular cross section, is evaluated as: $\lambda = \sqrt{12}L/h$.

Table B1. Maximum axial load from the 40 experimental tests R_{Exp} and related NLNAs R_{Mj} for the different structural models M_j (j=1-9).

Ref. [*]	**Exp. test**	**Type**	**λ [-]**	R_{Exp} **[kN]**	R_{Mj} **[kN]**								
					M_1	M_2	M_3	M_4	M_5	M_6	M_7	M_8	M_9
[24]	2L20-30	*B*	15	750.0	910.9	910.9	916.2	728.3	742.5	742.5	691.6	694.3	694.6
	2L20-60			700.0	978.8	978.8	985.5	734.8	735.8	744.0	736.4	736.4	739.5
	2L8-120R			1092.0	1587.0	1587.0	1587.0	1087.3	1090.9	1090.1	1152.7	1152.7	1152.7
	4L8-30			1100.0	1351.0	1351.0	1353.0	1110.9	1110.9	1110.9	1032.9	1032.9	1032.9
	4L20-120			900.0	1037.0	1037.0	1046.0	787.5	787.5	787.5	826.1	830.7	830.7
	4L8-120R			1247.0	1608.0	1608.0	1608.0	1211.3	1211.3	1211.3	1319.5	1319.5	1319.5
[27]	C000	*A*	17	559.6	611.6	611.6	611.6	545.1	545.1	545.1	560.6	560.6	560.6
	C020	*B*		327.3	396.0	396.0	402.9	319.9	336.9	338.0	325.7	328.5	329.0
	B020		52	271.5	298.6	298.6	308.6	219.2	227.2	227.2	257.0	263.7	263.7
	RL300		56	474.3	334.0	351.0	351.0	381.4	395.5	395.5	414.9	423.3	423.3
[28]	A-17-0.25	*B*	48	1181.4	1273.0	1273.0	1307.0	1322.1	1322.1	1346.4	1367.4	1367.4	1393.9
	C-31.7-0.25		94	333.4	207.4	219.6	219.6	224.8	262.8	262.8	248.4	280.1	280.1
[22]	3.3	*B*	59	782.6	827.3	827.3	835.9	787.5	787.5	809.4	856.4	856.4	866.5
	5.1			735.5	745.6	745.6	793.5	725.4	725.4	762.1	810.8	810.8	853.8
	4.1		88	367.7	297.7	346.8	346.8	210.9	403.0	403.0	397.5	391.7	455.7
[29]	N30-10.5-C0-3-30	*C*	68	16.6 (280)[*1]	11.6	11.9	11.9	23.5	23.5	24.6	16.2	16.6	17.6
	H60-10.5-C0-1-30			17.2 (412)[*1]	13.9	13.9	13.9	17.1	17.1	16.4	17.9	17.9	20.5
[30]	III	*A*	74	343.2	341.8	341.8	341.8	332.4	332.4	332.4	347.3	347.3	347.3
	Va			684.5	603.6	662.3	744.4	608.6	608.6	608.6	680.7	680.7	680.7
	2		83	235.4	197.4	217.7	217.7	191.2	224.5	224.5	216.2	236.8	247.3
	I		104	264.8	259.9	259.9	259.9	252.4	252.4	251.4	258.0	258.0	258.0
	VI		106	392.3	361.0	361.8	361.8	327.3	327.9	327.9	363.2	363.2	363.2
	15		136	549.2	509.4	509.4	509.4	394.4	394.4	394.4	560.3	560.3	560.3
	3		137	666.9	511.4	511.4	511.4	456.6	456.6	393.6	563.4	563.4	563.4
	8	*B*	83	235.4	197.4	217.7	217.7	191.2	224.5	224.5	216.2	236.8	247.3
	9		135	205.9	163.7	184.5	184.5	205.3	205.3	205.3	161.1	205.9	208.7
	12			112.8	153.5	153.5	172.5	114.7	114.7	151.5	115.2	112.2	176.8
	6		137	225.6	185.7	204.1	204.1	153.4	223.2	223.2	187.4	227.6	244.0
[23]	24D-2	*D*	104	198.4	184.6	184.6	184.6	188.0	192.1	192.1	192.8	192.8	192.8
	15E-2	*A*	139	161.0	121.4	121.9	121.9	127.0	130.0	130.0	129.3	129.3	129.3
[26]	S28	*B*	167	44.0	53.9	53.9	58.6	55.4	54.9	54.9	49.9	49.9	55.8
	S30			48.0	54.9	54.9	59.8	56.1	56.1	60.6	58.5	53.4	66.7
	S25		200	36.0	39.5	39.5	43.6	31.2	37.8	42.0	42.3	42.3	49.0
[25]	5	*A*	208	72.7	67.6	67.6	67.8	53.9	53.9	53.9	78.7	78.7	78.7
	6			72.2	70.3	70.3	70.6	52.0	52.0	52.0	82.3	82.3	82.3
	17A		225	31.9	32.7	32.7	32.8	20.1	26.0	24.1	37.1	37.1	37.1
	20		243	37.9	29.1	30.2	30.2	27.4	27.4	27.4	39.8	39.8	39.8
	18			33.9	29.1	30.2	30.2	24.4	24.4	24.4	39.8	39.8	39.8
	8		274	31.9	26.6	26.6	26.6	23.3	23.3	23.3	31.0	31.0	31.0
	7			29.9	27.6	27.6	27.6	20.6	20.6	20.6	32.3	32.3	32.3

(-)*[1] Constant value of the axial load applied to the column during the experimental test.

Table B2. Outcomes for the observed values of resistance model uncertainty $\vartheta = R_{Exp} / R_{Mj}$ related to the 40 slender columns considered for the investigation conditional to the specific structural model M_j (j=1-9).

Ref. [*]	**Exp. test**	**Type**	**λ [-]**	ϑ **[-]**								
				M_1	M_2	M_3	M_4	M_5	M_6	M_7	M_8	M_9
[24]	2L20-30	*B*	15	0.82	0.82	0.82	1.03	1.01	1.01	1.08	1.08	1.08
	2L20-60			0.72	0.72	0.71	0.95	0.95	0.94	0.95	0.95	0.95
	2L8-120R			0.69	0.69	0.69	1.00	1.00	1.00	0.95	0.95	0.95
	4L8-30			0.81	0.81	0.81	0.99	0.99	0.99	1.06	1.06	1.06
	4L20-120			0.87	0.87	0.86	1.14	1.14	1.14	1.09	1.08	1.08
	4L8-120R			0.78	0.78	0.78	1.03	1.03	1.03	0.95	0.95	0.95
[27]	C000	*A*	17	0.91	0.91	0.91	1.03	1.03	1.03	1.00	1.00	1.00
	C020	*B*		0.83	0.83	0.81	1.02	0.97	0.97	1.00	1.00	0.99
	B020		52	0.91	0.91	0.88	1.24	1.19	1.19	1.06	1.03	1.03
	RL300		56	1.42	1.35	1.35	1.24	1.20	1.20	1.14	1.12	1.12
[28]	A-17-0.25	*B*	48	0.93	0.93	0.90	0.89	0.89	0.88	0.86	0.86	0.85
	C-31.7-0.25		94	1.61	1.52	1.52	1.48	1.27	1.27	1.34	1.19	1.19
[22]	3.3	*B*	59	0.95	0.95	0.94	0.99	0.99	0.97	0.91	0.91	0.90
	5.1			0.99	0.99	0.93	1.01	1.01	0.97	0.91	0.91	0.86
	4.1		88	1.24	1.06	1.06	1.74	0.91	0.91	0.93	0.94	0.81
[29]	N30-10.5-C0-3-30	*C*	68	1.43	1.39	1.39	0.71	0.71	0.67	1.02	1.00	0.94
	H60-10.5-C0-1-30			1.24	1.24	1.24	1.01	1.01	1.05	0.96	0.96	0.84
[30]	III	*A*	74	1.00	1.00	1.00	1.03	1.03	1.03	0.99	0.99	0.99
	Va			1.13	1.03	0.92	1.12	1.12	1.12	1.01	1.01	1.01
	2		83	1.19	1.08	1.08	1.23	1.05	1.05	1.09	0.99	0.95
	I		104	1.02	1.02	1.02	1.05	1.05	1.05	1.03	1.03	1.03
	VI		106	1.09	1.08	1.08	1.20	1.20	1.20	1.08	1.08	1.08
	15		136	1.08	1.08	1.08	1.39	1.39	1.39	0.98	0.98	0.98
	3		137	1.30	1.30	1.30	1.46	1.46	1.69	1.18	1.18	1.18
	8	*B*	83	1.19	1.08	1.08	1.23	1.05	1.05	1.09	0.99	0.95
	9		135	1.26	1.12	1.12	1.00	1.00	1.00	1.28	1.00	0.99
	12			0.73	0.73	0.65	0.98	0.98	0.74	0.98	1.01	0.64
	6		137	1.21	1.11	1.11	1.47	1.01	1.01	1.20	0.99	0.92
[23]	24D-2	*D*	104	1.07	1.07	1.07	1.06	1.03	1.03	1.03	1.03	1.03
	15E-2	*A*	139	1.33	1.32	1.32	1.27	1.24	1.24	1.25	1.25	1.25
[26]	S28	*B*	167	0.82	0.82	0.75	0.79	0.80	0.80	0.88	0.88	0.79
	S30			0.87	0.87	0.80	0.86	0.86	0.79	0.82	0.90	0.72
	S25		200	0.91	0.91	0.83	1.15	0.95	0.86	0.85	0.85	0.73
[25]	5	*A*	208	1.08	1.08	1.07	1.35	1.35	1.35	0.92	0.92	0.92
	6			1.03	1.03	1.02	1.39	1.39	1.39	0.88	0.88	0.88
	17A		225	0.98	0.98	0.97	1.59	1.23	1.32	0.86	0.86	0.86
	20		243	1.30	1.25	1.25	1.38	1.38	1.38	0.95	0.95	0.95
	18			1.16	1.12	1.12	1.39	1.39	1.39	0.85	0.85	0.85
	8		274	1.20	1.20	1.20	1.37	1.37	1.37	1.03	1.03	1.03
	7			1.08	1.08	1.08	1.45	1.45	1.45	0.93	0.93	0.93

FIGURES

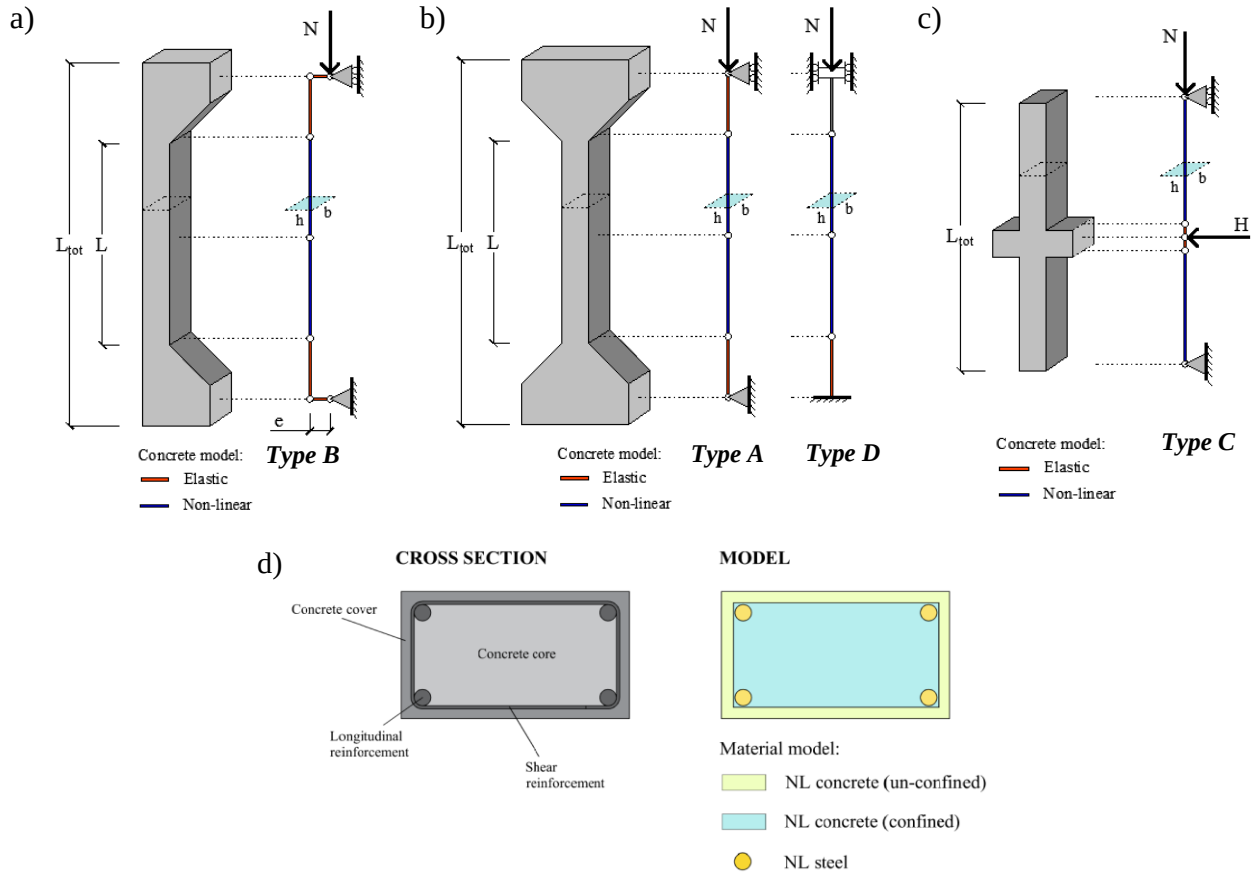

Fig. 1. Static schemes for the typical experimental tests and schematization of the numerical models and typical cross sections of the reinforced concrete columns.

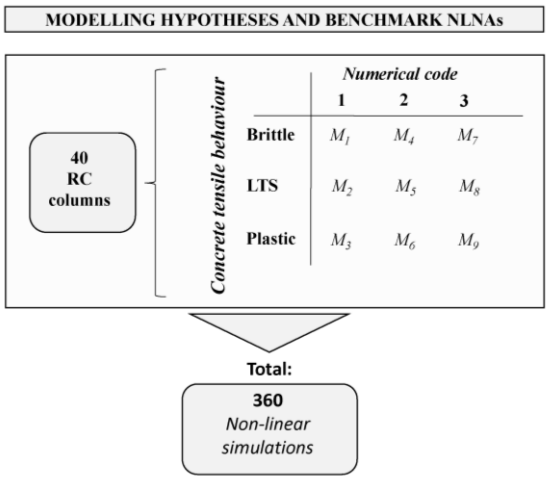

Fig. 2. Differentiation between the plausible modelling hypotheses for non-linear analysis of RC columns.

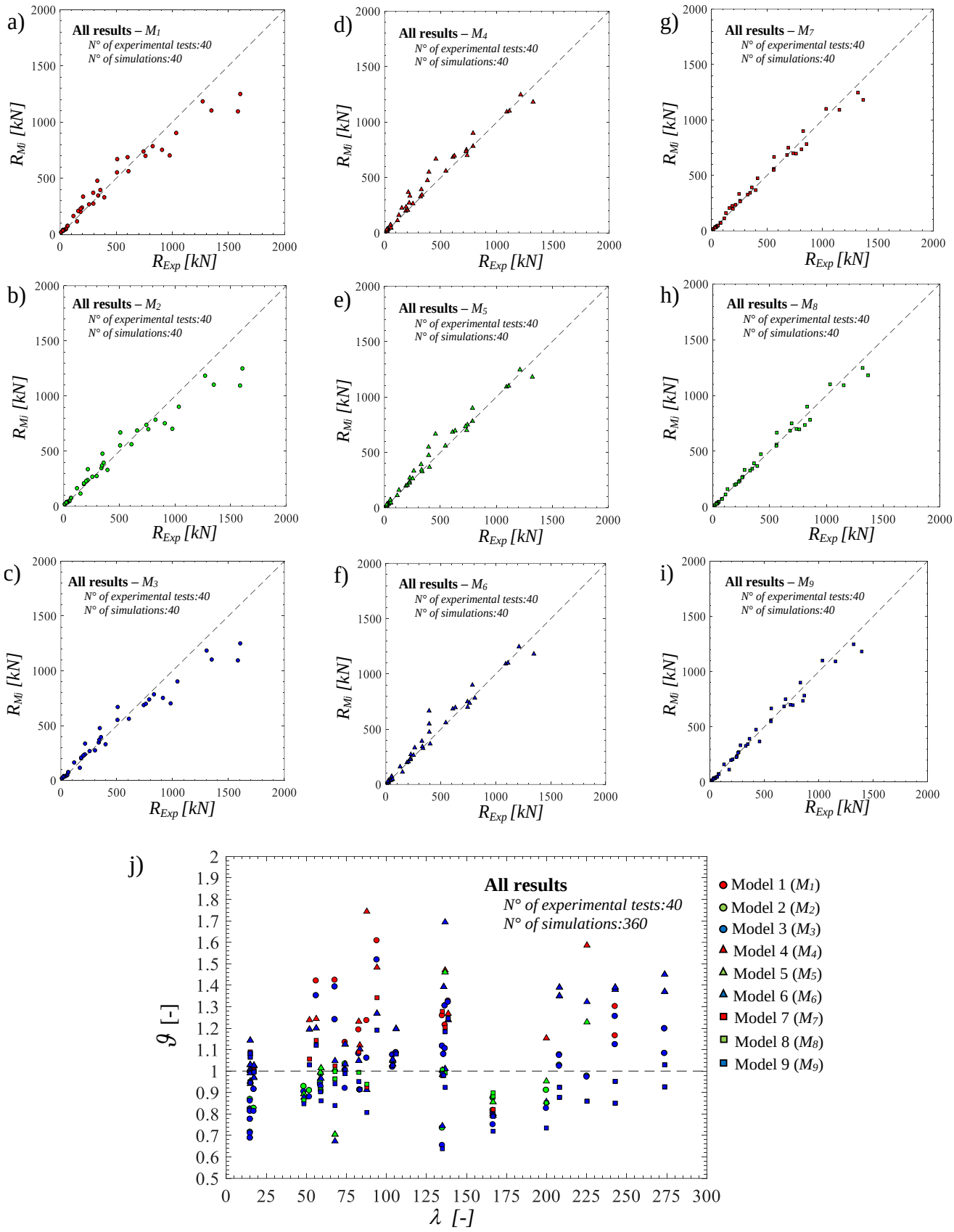

Fig. 3. Comparison between the outcomes of the 40 experimental tests of [22]-[30] R_{Exp} and the numerical simulations R_{Mj} related to the 9 modelling hypotheses (a-i); Representation of the sample of the resistance model uncertainty random variable $\vartheta = R_{Exp}/R_{Mj}$ for all the structural models M_j (j=1-9) with reference to the different values of slenderness λ.

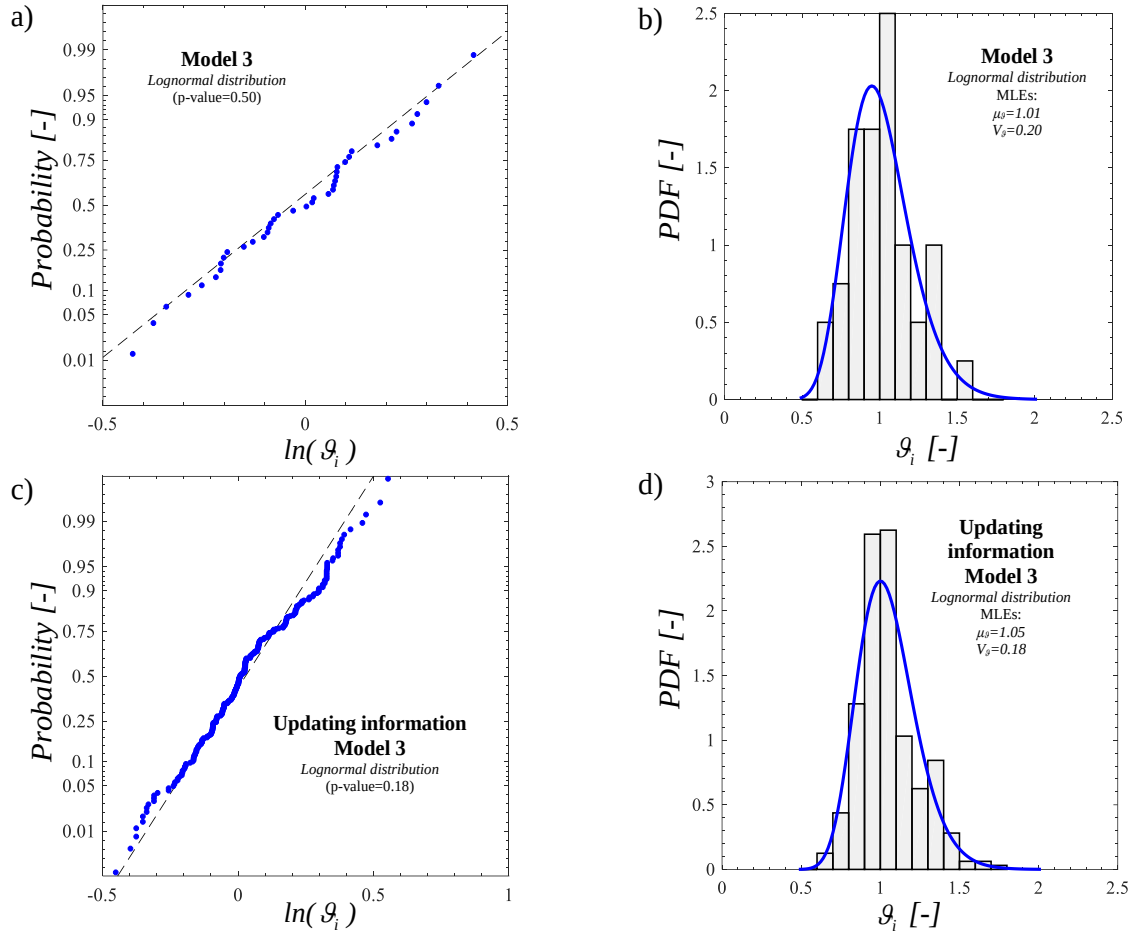

Fig. 4. Probability plot of $ln(\vartheta_i)$ for the Model 3 (a) and its updating information (c); Relative frequency histogram and lognormal PDF of the ratio ϑ_i for the Model 3 (b) and its updating information (d).

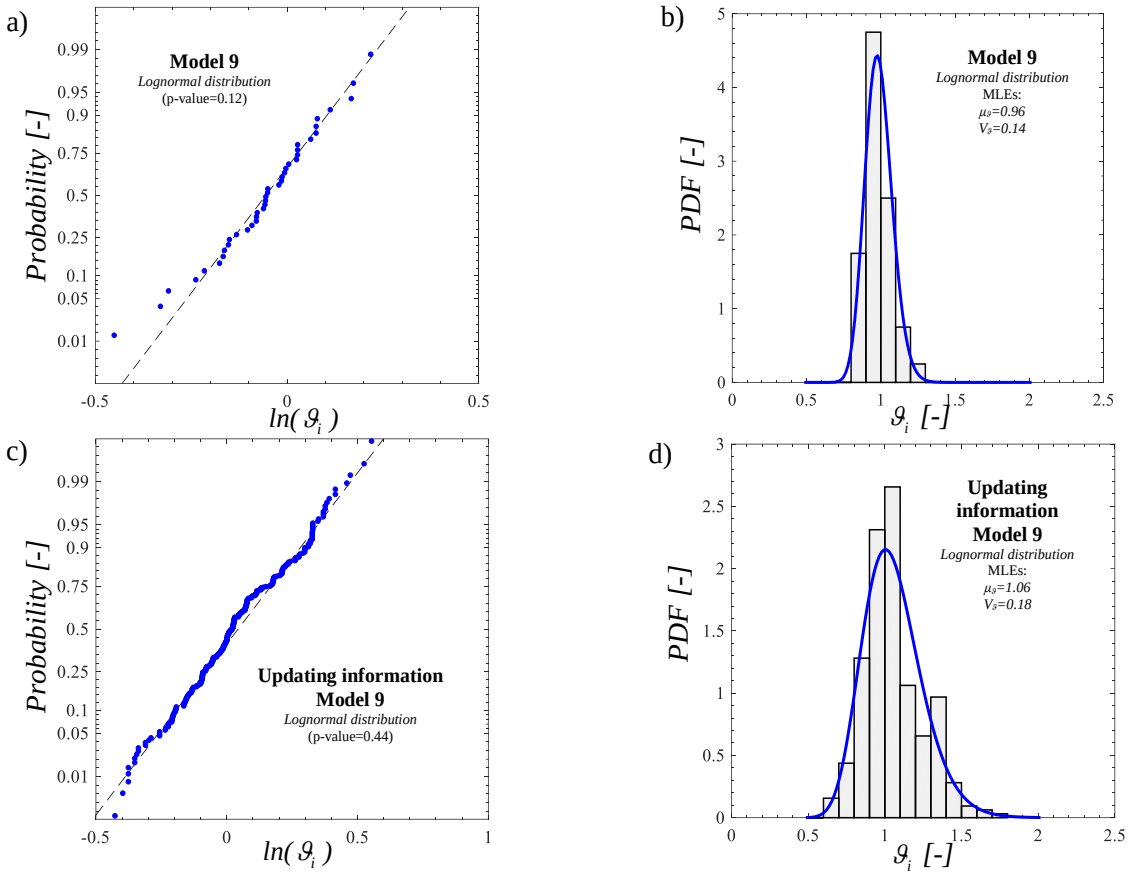

Fig.5. Probability plot of $ln(\vartheta_i)$ for the Model 9 (a) and its updating information (c); Relative frequency histogram and lognormal PDF of the ratio ϑ_i for the Model 9 (b) and its updating information (d).

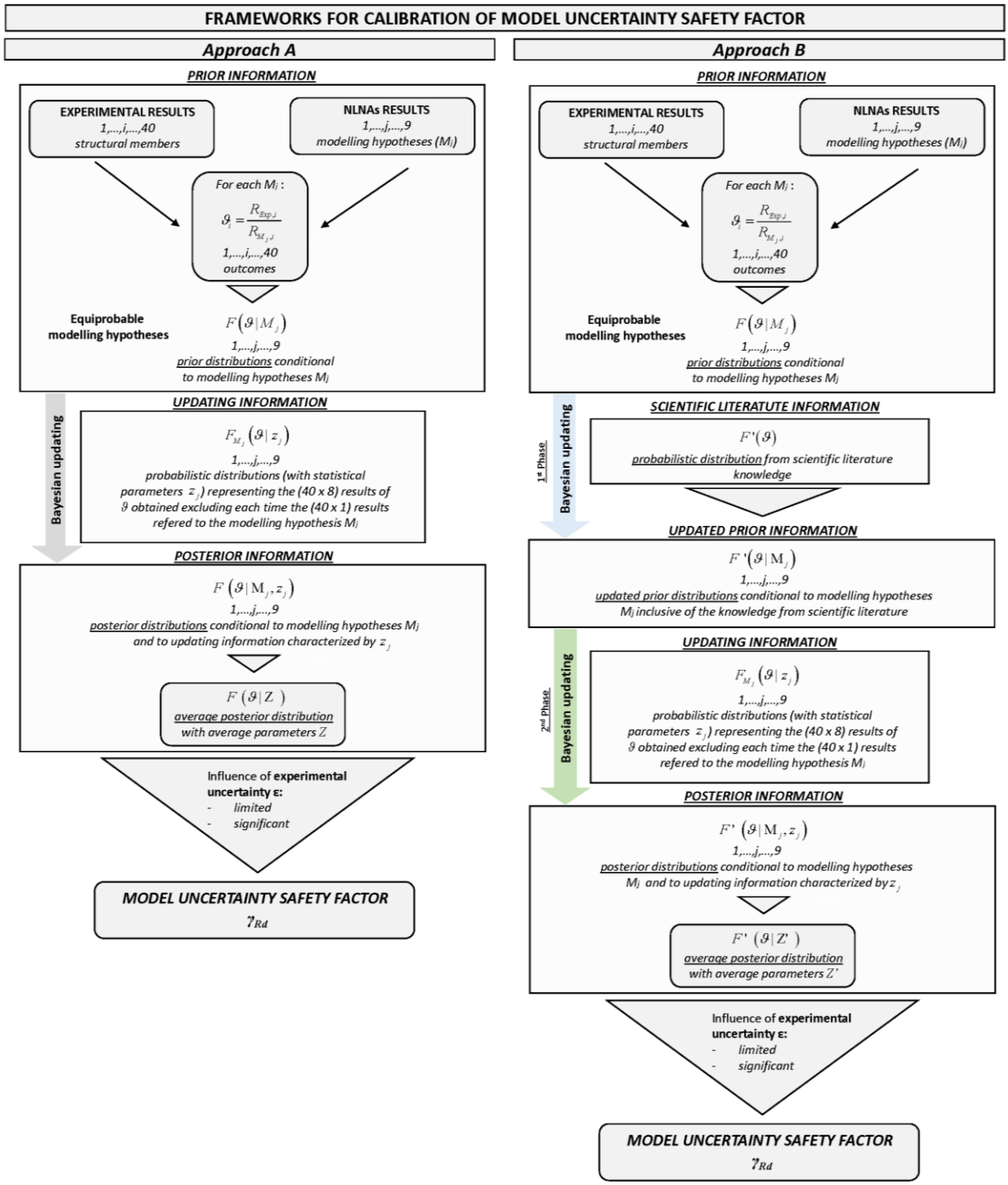

Fig. 6. Flow-chart representing the *Approach A* and *the Approach B* for the estimation of the model uncertainty safety factor.

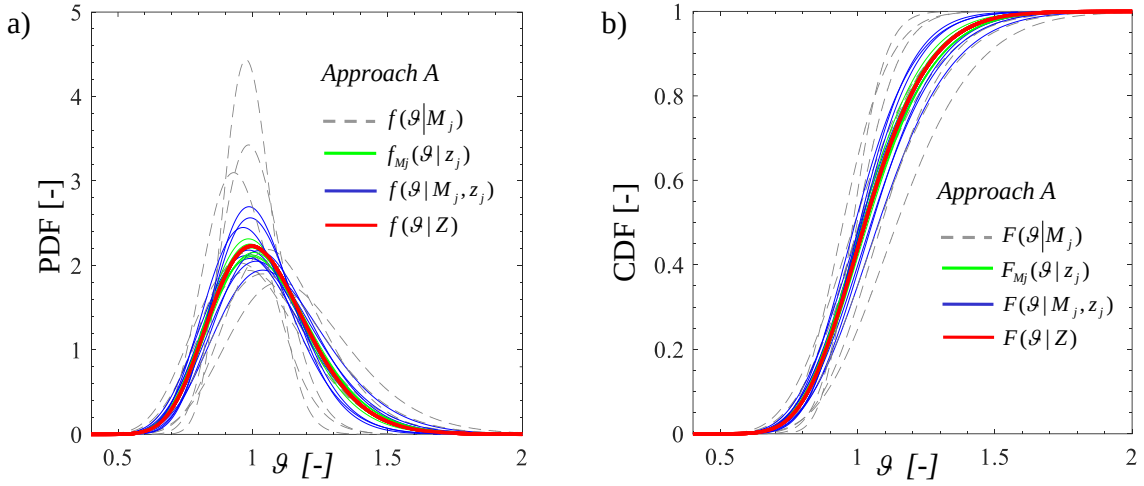

Fig. 7. Probabilistic distributions of prior, posterior and updating information PDFs (a) and CDFs (b) – *Approach A.*

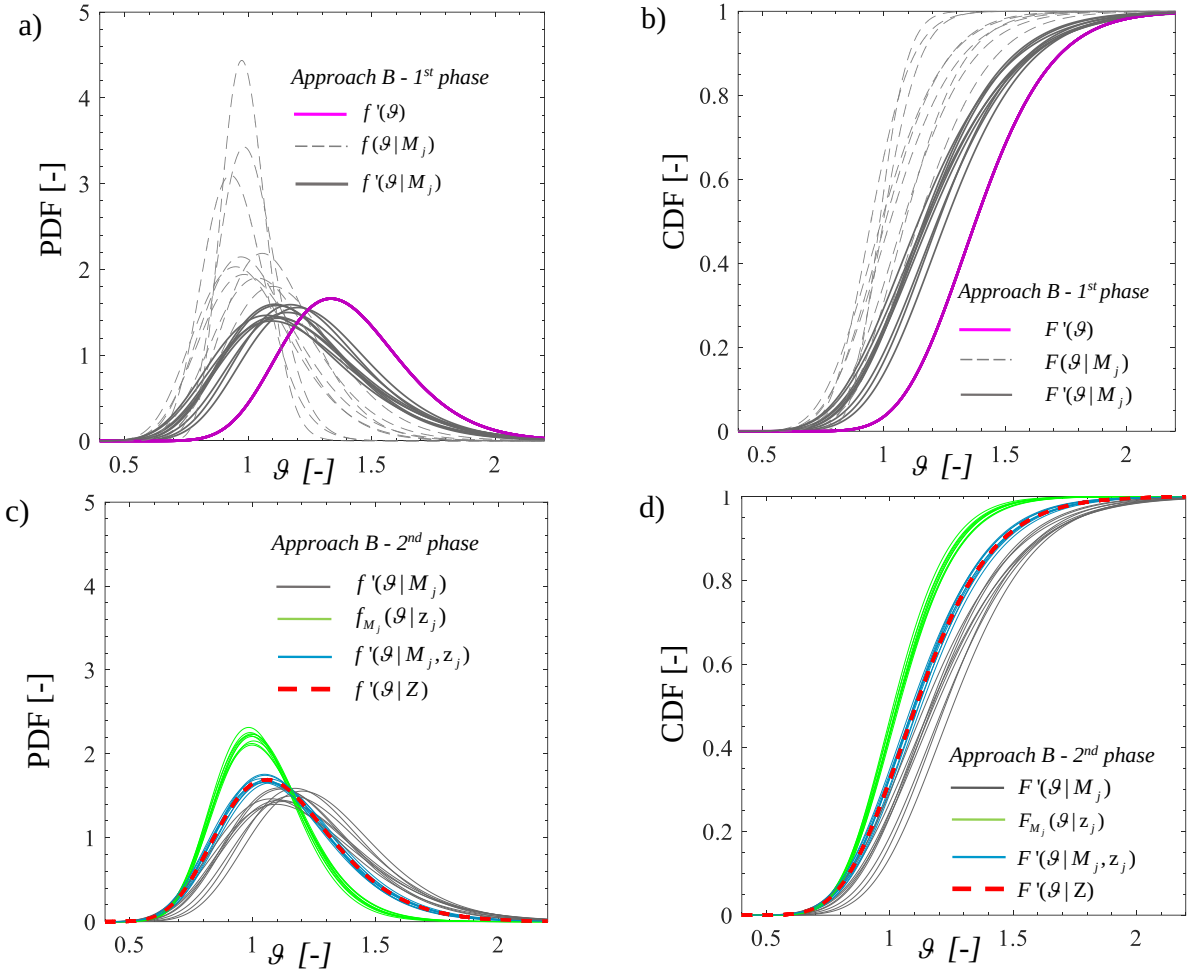

Fig. 8. Probabilistic distributions related to prior, posterior and updating information related to 1st phase PDFs (a) and CDFs (b), and 2nd phase PDFs (c) and CDFs (d) – *Approach B.*

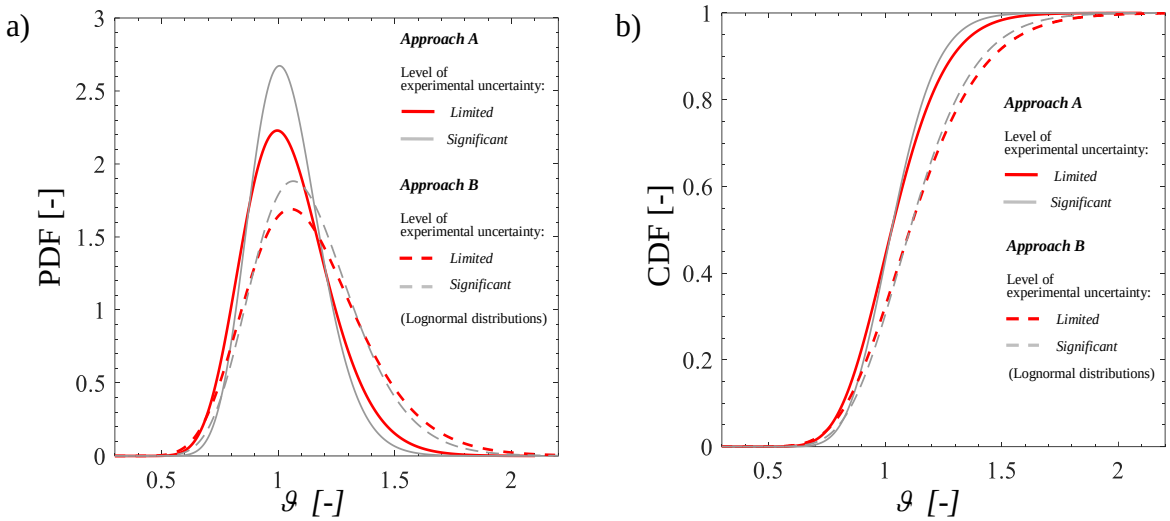

Fig. 9. Comparison between the lognormal probabilistic distributions, PDFs (a) and CDFs (b), related to *Approach A* and *B*.